North Carolina Agricultural and Technical State University

Aggie Digital Collections and Scholarship

Spring 2015

Investigation Of Biomechanical Risk Factors Of Medial Tibial Stress Syndrome Through Finite Element Analysis

Robert Allen Wesley
North Carolina Agricultural and Technical State University

Follow this and additional works at: https://digital.library.ncat.edu/theses

Recommended Citation

Investigation of Biomechanical Risk Factors of Medial Tibial Stress Syndrome through Finite

Element Analysis

Robert Allen Wesley

North Carolina A&T State University

A thesis submitted to the graduate faculty

in partial fulfillment of the requirements for the degree of

MASTER OF SCIENCE

Department: Chemical, Biological, and Bioengineering

Major: Bioengineering

Major Professor: Dr. Matthew McCullough

Greensboro, North Carolina

2015

The Graduate School

North Carolina Agricultural and Technical State University

This is to certify that the Master's Thesis of

Robert Allen Wesley

has met the thesis requirements of

North Carolina Agricultural and Technical State University

Greensboro, North Carolina

2015

Approved by:

_____   _____

Dr. Matthew McCullough   Dr. Yeoheung Yun
Major Professor   Committee Member

_____   _____

Dr. Stephen Knisley   Dr. Narayan Bhattarai
Department Chair   Committee Member

_____

Dr. Sanjiv Sarin
Dean, The Graduate School

Biographical Sketch

Robert Allen Wesley has a passion for research and intellectual challenge. In 2008, he started working in the environmental health and safety laboratory at East Tennessee State University. He was given little training and was self-taught in spectroscopy and spectrophotometry while analyzing water samples collected from local rivers and creeks. In his two years of working for the university, he taught himself the principles of furnace and flame atomic absorption and wrote a user's manual for the laboratory instrumentation.

In 2010, he transferred to Tennessee Technological University to start his pursuit of a chemical engineering bachelor's degree. It took two years to become fully immersed in the program. He served as Community Service Chairman and Vice President of the American Institute for Chemical Engineers chapter. In 2012, he researched the potential of 5th generation polyamidoamine dendrimers as nanocarriers for pharmaceuticals, with the focus of analyzing biocompatibility and cytotoxicity with Dr. Robby Sanders. In 2013, he worked under Dr. Cynthia Rice, operating fuel cell test stations, preparing formic acid solution, analyzing the performance data collected from fuel cells having a palladium catalyst, and learning the principles of electrochemical impedance spectroscopy.

Nearing graduation from Tennessee Technological University, he interviewed with several of the professors of the Chemical, Biological, and Bioengineering department of North Carolina A&T State University. Despite the campus being on lockdown due to a suspected gunman, he chose to willingly enter the building in hopes that his interviews with the professors would be well worth the risk. He met one of his influential professors that day, Dr. Matthew McCullough. Robert interviewed with Dr. McCullough two more times before joining Dr. McCullough's computational biomechanics research team.

Dedication

I dedicate this to my parents, Steve and Kittie Wesley. Your support has been more than any son could ever ask for. The love, patience, and understanding you have shown me have known no bounds. I would not have had the confidence to pursue this degree without you.

Acknowledgments

I would like thank my committee for guiding me through graduate school. Dr. Narayan Bhattarai, Dr. Matthew McCullough, and Dr. Yeoheung Yun are three of the most influential professors of my academic career. Thank you for being my committee. Thank you for your mentorship. I would like to thank the Chemical, Biological, and Bioengineering staff of North Carolina A&T State University for their support and the opportunities provided.

Table of Contents

List of Figures

List of Tables

Abstract

Medial tibial stress syndrome (MTSS) is an overuse injury in the lower extremity associated with endurance running. MTSS is a palpitation of pain of at least 5 centimeters along the medial tibia with possible microfractures in the tibia. The various risk factors which may lead to the development of MTSS are body mass index, over pronation, heel striking, level of shod in the running shoe, type and angle of running surface, high volume training, age, gender, stride length, range of motion, and calf girth. Few investigations have been made to limit these risk factors through the utilization of finite element analysis (FEA). This study investigates the likelihood of MTSS developing and the possibility of microfractures in the tibia under varying conditions of pronation degree, body mass index, material property, and gait phase. FEA was used in order to measure the von Mises stress of 24 human tibia models. The simulations were run for three main phases of gait "impact", "mid-stance", and "push-off". The risk factors under investigation were intrinsic in nature, which are over pronation (OP) and body mass index (BMI). Forces were input for 2 male subjects running at 8 miles per hour on a flat surface. Simulations were run for isotropic and orthotropic tibia models with "normal pronation and normal BMI", "over pronation and normal BMI", "normal pronation and high BMI", and "over pronation and high BMI". FEA revealed that the combination of over pronation and high BMI consistently had the greatest von Mises stresses throughout each phase of gait for isotropic and orthotropic tibia models. Statistical results show that material properties had the greatest effect on the measured von Mises stress followed by pronation degree, gait phase, and BMI. A normality test with a confidence interval of 95% proved that the distribution of von Mises stress across was acceptable for all models with P=0.130. Factorial ANOVA was run for gait phase,

BMI, pronation degree, and material property, which also confirmed the greatest effects on von

Mises stress are material property, pronation degree, gait phase, and then BMI.

CHAPTER 1

Introduction

Medial tibial stress syndrome (MTSS) is one of the most common injuries experienced by running and jumping athletes. As a condition it is often labeled as "shin splints" (SS) a term that dates back over 40 years, and describes leg pain which occurred in athletes with MTSS[1]. MTSS however, specifically refers to pain on the posteromedial tibial border occurring during exercise. The terms are not interchangeable as "shin splints" can refer to a general sensation of pain proximal to the shin. Exams have reported pain on palpation of the tibia over a length of at least 5 cm. Many studies have attempted to clarify the origins of this condition. While there is disagreement about ongoing studies, researchers do agree that MTSS is caused by bony resorption outpacing bone formation in the tibial cortex as evident in several studies describing MTSS findings on bone scan, magnetic resonance imaging (MRI), high-resolution computed tomography (CT) scan and dual energy x-ray absorptiometry [2].

The time lag between scientific understanding and practical application appears to be pronounced in the area of tibial stress injuries. While this may reflect the non–life-threatening nature of the injury, the belated dissemination of more progressive management techniques implies that rest from weight-bearing activity is an acceptable treatment. However, not only can tibial stress injuries be highly disruptive to a regular fitness regimen, these injuries end careers of competitive athletes and military personnel. Furthermore, in a world that is becoming increasingly focused on 'sport as business', in which readiness to participate is an economic consideration. Prolonged periods of recovery from injury have additional negative repercussions for athletes [3].

The incidence of MTSS is reported between 4% and 35% in military personnel and athletes [2]. Medial tibial stress syndrome accounts for about 10 to 15% of all running injuries. It has also been found that up to 60% of all conditions that cause leg pain in athletes have been attributed to SS. SS, referring to pain and discomfort in the leg from repetitive running on hard surfaces or forcible excessive use of foot flexors, accounts for 6% to 16% of all running injuries and is responsible for as much as 50% of all lower leg injuries reported in select populations [4]. Recent studies report up to a 35% incidence of MTSS in actively training military recruits and 13% in civilian runners [5]. MTSS accounts for 17.3% of all injuries in runners and accounts for 22% of all injuries in aerobic dancers [6]. In spite of such significant numbers, little data is available on the economic impact of these conditions.

1.1 Anatomy and Physiology

The term "shin splints" is an encompassing term for general shin pain, whereas this paper is focused on the medial section of the tibia. MTSS is a common diagnosis given when someone is suffering from pain in the front of their legs or more specifically the medial portion of the tibia and is often associated with running. Alternative terms to SS have been proposed over the years. Mubarak et al popularized the term medial tibial stress syndrome, a condition that leads to pain in the posteromedial aspect of the distal two thirds of the tibia [7].

A sudden increase in running mileage, and/or the beginning of a new running activity may also cause SS, which worsen when running downhill. The pain associated with MTSS, as opposed to posterior tibial stress syndrome or lateral tibial stress syndrome, is a deeper, achy pain, which can lead to a slapping foot while running. Once an athlete stops running, the pain may remain for 15 minutes. If pain continues, it may be associated with Exertional Compartment syndrome, which is described as feeling pressure pushing towards the lateral side of the lower

leg [9]. The cause of the pain in this scenario is an increase in pressure in the anterior

compartment of the leg. The affected compartment is between the tibia and fibula (the two bones

in the lower leg) and a thick layer of fascia around the posterior tibialis muscle. Within this

compartment lies the tibialis anterior muscle as well as the muscles that extend your toes. When

running, these muscles help to lift (dorsiflex) one's foot and toes allowing for ground clearance

during the swing phase. These muscles also lower one's foot and toes to the ground after heel

strike at the beginning of the stance phase of running. Muscle contraction increases the need for

blood in the area. This increased blood supply to the muscle in turn increases the size of the

muscle. This process is normal and usually goes unnoticed, however if the size or volume of the

muscle increases too much, especially when the muscle is held tight like in the anterior

compartment, it results in an increase in pressure causing pain. The pressure in the anterior

compartment can get high enough that it affects the muscles ability to function often causing foot

slapping while running. During this condition, the aforementioned muscles can no longer control

the lowering of the foot to the ground after heel contact, so the foot slaps uncontrollably. If the

pressure continues to increase, it can even disable the sensory nerve contribution to the skin

between the first two toes [9].

1.2 Mechanism of Injury

Once the soleus muscle gets tight and/or overworked from sudden increases in running

mileage or when starting a new activity, the muscle begins to tug at the attachment along the

medial border of the tibia. This tugging causes the pain on the inside of the shin. The body

responds by creating scar tissue along the attachment for reinforcement. This reaction only

causes the muscle to become tighter and places even more stress along the attachment at the shin.

This vicious cycle of pain and tightening will continue until one seeks treatment, stops the

activity, or modifies the activity to provide time for proper healing [10]. The pain is sharp and decreases significantly once running stops, and after 15 minutes is almost gone. Shins are tender or painful to the touch along the middle third of the inside of the tibia [11]. If the pressure continues to increase, it can even disable the sensory nerve contribution to the skin between the first two toes [9]. MTSS usually begins with the onset of a new running activity and/or a sudden or rapid increase in mileage. An increase in body weight and running on hard surfaces has also been known to lead to this type of shin pain. The pain is caused by the soleus muscle that attaches to the tibia along its inside border [11].

Hubbard et al., concluded that the cause of MTSS is not attributed to a single internal or external factor [12]. For example, as much as 70% of runners over pronate, however between 40 and 50% of excessive pronators do not have overuse injuries, such as MTSS [13,14]. Literature has also noted that "experts do not agree upon the cause of MTSS", making it difficult to prevent [15, 17-22]. In spite of the complexities associated with the onset of MTSS researchers and physicians have agreed upon a general set of possible causative factors including but not limited to:

A: Tibialis Posterior Separation from the Bone – Pain is caused by traction of the tibialis posterior muscle origin on the interosseus membrane and tibia [23, 24]. This is one of the original theories regarding causes for MTSS, however, researchers have been skeptical of the tibialis posterior's involvement as the location of the muscle origin is quite a distance away from the location of pain [25].

B: Periostitis – This refers to inflammation of the layer of connective tissue that surrounds the tibial bone (the periosteum). Recently research has shown increased bone stress or musculotendinous breakdown before MTSS [26]. Many believe the main cause of MTSS

involves underlying periostitis of the tibia due to tibial strain when under a load. However, new evidence indicates that a spectrum of tibial stress injuries is likely involved in MTSS, including tendinopathy, periostitis, periosteal remodeling, and stress reaction of the tibia. Dysfunction of the tibialis posterior, tibialis anterior, and soleus muscles are also commonly implicated. These various tibial stress injuries appear to be caused by alterations in tibial loading, as chronic, repetitive loads cause abnormal strain and bending of the tibia. Although sometimes composed of different etiologies, MTSS and tibial stress fractures may be considered on a continuum of bone–stress reactions [27].

C: Traction of the Deep Crural Fascia – A fairly recent theory on the causation associated with MTSS is traction, or pulling, of the deep crural fascia within the lower leg. Fascia is connective tissue involved with multiple structures within the body, and sometimes fuses with the bony structures [28]. Traction-induced injury, related to muscles of the superficial and deep posterior compartments, has been implicated as the cause of medial tibial stress syndrome (MTSS) with symptoms commonly occurring in the distal third of the posteromedial tibia. Research into the anatomical arrangement of these structures has been inconclusive. The deep crural fascia (DCF) has been implicated as a cause of traction-induced injury in MTSS but not fully researched [17].

1.2.1 Diagnosis

MTSS is diagnosed primarily based on physical examination with CT and MRI [9]. MTSS is often associated with the muscles surrounding the tibia, but there is also a risk of stress microfractures developing in the tibia. The association of MTSS with microfractures is under investigation but has not been confirmed due to the lack of radiologic findings. MRI can reveal stress microfractures in the bone [9]. When attempting to diagnose a tibia stress fracture through

MRI and CT, the lack of a fracture leads to the assumption of MTSS. It offers the most accurate description of the involved anatomy and presumed pathophysiology of this most common form of tibial stress injury. The hallmark of the physical examination in MTSS is palpable tenderness over a 4 to 6 cm area at the posteromedial margin of the middle to distal third of the tibia. Passive stretch of the soleus, heel rises, and unilateral hopping may reproduce pain [7].

In clinical practice, graded running, as well as strengthening and stretching exercises for the calf muscles are frequently prescribed for MTSS [30, 31]. Waldorff et al., concluded that graded running in itself could strengthen the tibial cortex by increasing the remodeling of the tibia and increased resorption of micro-damage [32-34]. While very few studies have been published on the effect of stretching for MTSS, research has shown that stretching may help in the recovery stage; there is no fast cure to medial tibial stress syndrome. A doctor or physical therapist will often recommend a stretching regimen, icing of the affected area, and wrapping the lower leg with an Ace bandage to reduce inflammation [35-38].

In-shoe foot orthotic devices are designed to support foot structures and limit abnormal and potentially harmful motions that may lead to lower extremity pain and dysfunction. Orthotic inserts or arch taping are thought to correct pes planus and limit pronation, thereby reducing the incidence of, preventing exacerbation of, and sometimes assisting in the recovery from tibial overuse injuries. Pes planus has been associated with an increased incidence of shin injury and tibial stress fracture. Similar to hyperpronation, the effect is likely to be one resulting from excessive medial tibial torsion following exaggerated internal rotation during the stance phase of a stride [3].This is important because excessive bone strain and strain rates are associated with microdamage and stress fracture of bone. Hence, orthotics may be an effective prevention and treatment strategy for strain injuries [39].

Sports compression stockings are used frequently in the Netherlands to treat MTSS [40]. A sports compression stocking provides direct compression of the tibia and via the surrounding soft tissues, especially during intermittent loading. Compression of bony tissue has been shown to promote the expression of bone remodeling genes, accelerating the healing process [41].

Excessive pronation of the foot while standing and female sex were found to be intrinsic risk factors in multiple prospective studies [42]. Other intrinsic risk factors found in single prospective studies are higher body mass index, greater internal and external ranges of hip motion, and calf girth. A previous history of MTSS is considered to be an extrinsic risk factor [29].

It is well understood that individuals with MTSS also show a reduced bone density in the tibia, which returns to normal with recovery [31]. Also it has been noted that both the soleus and tibialis anterior muscles have reduced activity in the lower leg, prior to injury, suggesting that strength of these muscles are likely affected when running [44]. An in depth investigation of the following biomechanical factors: pronation, range of motion, and foot strike, follows.

1.2.2 Pronation

The diagnosis of MTSS has been associated with a greater degree of foot pronation [45]. Foot pronation is a complex triplanar movement. Visually, it is characterized by a flattening of the Medial Longitudinal Arch (MLA) and an abduction of the calcaneus, a rotation of the extremity around the y-axis [14]. Bouche *et al*. hypothesized that large foot pronation induces tension on the tibial fascia at its insertion into the medial tibial crest and this could be one of the causes of MTSS [46]. Ankle joint eversion (pronation) has been associated with overuse locomotion injuries such as MTSS. The safe range of pronation is between 0° to 15°. An unsafe range (over pronation) is pronation of greater than 15°. Individuals with 2° to 4° of pronation

over the safe range typically have more repetitive stress injuries. As with the "normal pronation" sequence, the outside of the heel makes the initial ground contact. However, the foot rolls inward more than the ideal fifteen percent, which is called "overpronation." This means the foot and ankle have problems stabilizing the body, and shock isn't absorbed as efficiently. At the end of the gait cycle, the front of the foot pushes off the ground using mainly the big toe and second toe, which then must do all the work. [14].

Excessive navicular drop has been reported to predispose individuals to shin and MTSS [11, 48-50].Navicular Drop Test (NDT) is a test which quantifies the amount of foot pronation in runners [54]. It is intended to represent the sagittal plane displacement of the navicular tuberosity from a neutral position to a relaxed position in standing [53]. A navicular drop greater than 10 mm has a high risk of leading to MTSS [50,54].

1.2.3 Body Mass Index

In the Plisky *et al.* (2007) study, most MTSS injuries caused runners to miss 4 or less days from participation in practices or meets. Plisky et al., was unaware of any study that has reported time lost due to MTSS among high school runners. The findings, however, are comparable to other high school cross-country studies that reported that most injuries are minor and also suggested that most MTSS injuries were reported and managed early in the inflammatory stage [53].

Plisky et al., found that runners with higher BMI were more likely to incur MTSS. While this finding is consistent with other studies in military recruits BMI remains an equivocal risk factor for any type of lower extremity injury in other studies of high school, recreational, and recruit populations [53].

1.2.4 Range of Motion

Clinical measurement of range of motion is a fundamental evaluation procedure with ubiquitous application in physical therapy. Objective measurements of ROM and correct interpretation of the measurement results can have a substantial impact on the development of the scientific basis of therapeutic interventions [55]. Moen et al. (2012) reported after multivariate regression analysis, increased ankle plantar flexion, decreased internal hip range of motion and a positive navicular drop test were significantly associated with MTSS and defined as risk factors [11]. A higher BMI was shown to be a prognostic indicator for a longer time to full recovery. All other prognostic indicators such as a previous duration of symptoms, functional activity score, the symptom-free running distance at baseline, increased ankle plantar flexion, decreased internal range of hip motion and positive navicular drop test were not associated with time to recovery. A decreased range of hip internal rotation was found to be associated with MTSS in this study. The mechanism through which hip ranges of motion affect loading of the tibia is unclear. "Burne et al., speculated that increased internal hip range of motion caused a specific pattern of running, which could lead to increased loading of the posteromedial tibia [11]." Possibly, both increased and decreased internal hip range of motion influence running in such a way that the posteromedial tibia is loaded excessively [11].

1.2.5 Foot Strike

Because a runner's kinematics affects how external and internal forces are generated and withstood by the body, one should consider how differences in general running form may influence overall injury rates. Although running form has many components the impact of foot strike pattern is of special interest, on injury rates has not been previously studied is of special interest. Foot strikes vary, and there is no consensus on how to define and measure these

patterns. For this review, three categories of strike types that are prevalent among distance runners are defined: rearfoot strikes (RFS), in which the heel contacts the ground first (heel–toe running); forefoot strikes (FFS), in which the ball of the foot contacts the ground before the heel (toe–heel–toe running); and midfoot strikes (MFS), in which the heel and ball of the foot contact the ground simultaneously [56].

There are three major reasons to consider the biomechanics of foot strike pattern as it relates to MTSS/SS. First, how the foot strikes the ground involves disparate kinematics of the lower extremity. During a rearfoot strike, a runner usually lands with the foot in front of the knee and hip, with a relatively extended knee, and with a dorsiflexed, slightly inverted and abducted ankle; the runner then plantarflexes rapidly as the ankle everts just after impact. In contrast, a forefoot striking runner lands with a more flexed knee and plantarflexed ankle, usually making ground contact below the fourth or fifth metatarsal heads; the runner then simultaneously everts and dorsiflexes the foot during the brief period of impact, usually with more ankle and knee compliance. MFS landings are highly variable, but generally intermediate in terms of kinematics [56]. Second, different strike patterns generate contrasting kinetics, especially at impact. Midfoot striking can cause a broad range of impact peaks, from high to low, depending on ankle and knee compliance. Strike pattern also affects lower extremity joint moments, with forefoot strike landings causing higher net moments around the ankle in the sagittal plane and lower net moments around the knee and hip in both the sagittal and transverse planes. A final reason to study the relationship between foot strike pattern and injury rates is the growing popularity of running either barefoot or in minimal shoes that lack an elevated heel, contain no arch support, and have a thin, flexible sole [56]. All humans ran either barefoot or in minimal shoes before the invention of the modern running shoe in the 1970s [57]. Habitual shod runners, when asked to

run barefoot, instinctively land more toward the ball of the foot [58]. These and other sources of information, such as old coaching manuals, lead to the hypothesis that forefoot strike running may have been more common for most of human evolution. This hypothesis is relevant to the issue of running injury because if the foot evolved via natural selection to cope primarily with movements and forces generated during mostly forefoot rather than rearfoot strikes, then it follows that the body may be better adapted to forefoot strike running [59].

Faulty biomechanics can be very detrimental to the running athlete and result in pain. Biomechanics in the lower extremity hinge on the principle of the kinematic chain. The kinematic chain principle models extremities as composed of successively linked joint segments, which transfer forces and motions to the neighboring joints in a predictable pattern. In theory, when dysfunction occurs at a specific joint, the dysfunction will transfer to the following joint in sequence. When decreased motion occurs at the ankle during weight-bearing activity, both the knee and hip will feel the effects of the dysfunction and attempt to balance out the lost motion by increasing their ranges of motion. Attempts to compensate for the faulty mechanics of the ankle will cause the knee and hip to function in a new pattern. This transfer of faulty forces and movement can lead to injuries. This principle holds true for any joint in the chain during weight-bearing; therefore pelvic and hip range of motion are possible contributors to injury in the lower extremity [60].

Mburu et al. [48] recently used Taguchi methods to analyze systems of keyholes for cement fixation of the acetabular component of a total hip replacement. It is noteworthy that the Taguchi approach is not restricted to continuous response variables but can also be used on categorical variables, such as production method or boundary conditions [48].

1.3 Purpose

The purpose of this research is to model a human tibia under conditions that produce high stress and strains. This is important to study because such high stresses and strains could lead to microfractures and the development of MTSS. It is hypothesized that a combination of over pronation and high body mass index will yield a high stress and strain in the medial tibial region. A second hypothesis is that modeling the bone as an orthotropic material will yield higher stresses and or strains in the medial tibia region than models with isotropic material properties.

CHAPTER 2

Literature Review

2.1 In Vivo Methods

In vivo methods to determine risk factors are popular due to readily available and reliable kinematic data. An often cited weakness is the neglect of strain placed on the medial tibia which cannot be observed through traditional means. In epidemiology and in this review, a risk factor is a variable associated with the increased risk of developing an injury or illness. Therefore the risk factors discussed, are believed to increase the risk of developing MTSS.

Moen et al. [43] conducted a randomized multi-center study with three groups. The study population was comprised of athletes with a history of overuse injury. Each participant was randomly assigned to receive a specific intervention. Clinically trained sports physicians examined the athlete for complaints of MTSS during exercise and for suitability for inclusion. Moen used the exclusion criteria described by Edwards *et al.* in their recent review were used to identify stress fractures of the tibia and chronic exertional compartment syndrome (CECS). The athletes had to be involved in sport at least once a week. No significant differences between the intervention groups were found. Therefore, if MTSS is treated with a running program, no large additional effect of the two interventions can be expected. It should however, be noted that a graded running program has not been compared with a control group that rested in any study. It can only be assumed that graded running programs improve the density and strength of the tibia, and that rest does not have this effect [43]. Studies like the work of Moen et al. require a large number of subjects, researchers, and physicians. The time necessary to perform such project is much greater than for a project incorporating in silico methods. Challenges include coordinating tests around the athletes' and physicians' schedules, participant attrition due to pain, which has

an increasingly high probability as the duration of the study increases. As participants drop from a study like this, the opportunity to determine damage location in the tibia, cause of this damage, and whether it is damage muscle or bone tissue, is lost.

King, J. [59] analyzed data collected from The Runners and Injury Longitudinal Study (TRAILS), a large observational trial that examined the biomechanical, behavioral, physiologic, psychological, and clinical risk factors for runners who sustain an anterior knee pain overuse running injury. A secondary purpose was to determine the shared risk factors among runners who sustained any of the common overuse running injuries: anterior knee pain, iliotibial band friction syndrome, medial tibial stress syndrome, Achilles tendinitis, or plantar fasciitis. For this study, baseline kinematic, kinetic, anthropometric, and strength data, and data on injury status were used to compare selected biomechanical, physiological, and behavioral variables of runners. These runners were selected based on current injury, lack of injury, or had had a history of overuse injury [59]. 184 distance runners between the ages of 18 and 60 years old were recruited to TRAILS during a 6-month period. Male and female runners were enrolled who have been running injury free for the past 6 months. For this analysis, 159 TRAILS participants, whose gait, strength, and anthropometric data were available, were split into a "Never Injured" (N = 49), "Occasionally Injured" (N = 36), and "Frequently Injured" group (N = 74). The Never Injured group had not experienced an overuse running injury prior to the study and had remained injury free over the course of the study. The Occasionally Injured group had either 1) been injured prior to the study but not during the study, or 2) had been injured during the study, but not prior to the study. The Frequently Injured group had been injured prior to the study and during the study. Motion and force data were analyzed to determine lower extremity and motion parameters, and used as input into a musculoskeletal model to calculate knee joint forces [59].

The authors examined rearfoot biomechanics and knee-joint loads. Subjects ran in their normal training shoes at their average training speed on a 22.5 m runway while motion and force data was captured. Outcome variables included rearfoot motion parameters, tibial medial/lateral rotation, knee flexion/extension, timing between lower extremity segments, and vertical and anteroposterior ground-reaction forces [59]. This method collects a large amount of kinematic data to recreate a musculoskeletal model. The study was statistically justified out of the 184 research subjects, 25 were dropped from the study, roughly 14% of the subjects.

2.2 Computational Studies

Olesen et al. [60] built a musculoskeletal model of the lower extremitiy the AnyBody Modeling System. The model was based on cadaver data and included 38 muscles that were divided into 316 muscle fascicles, based on the line-of-action. A Hill-type muscle model with passive elasticity and force-length-velocity relationships was used. The model was driven through a gait cycle with kinematic and kinetic data from a gait experiment on a healthy male. The right foot was artificially rotated about an axis going from the calcaneus and through the 2nd metatarsal bone to simulate different degrees of pronation. The rotation went from 20° pronation to -5° supination, mimicking foot postures from highly pronated to slightly supinated. The simulations were run with increments of 5°. For each foot posture the muscle recruitment problem was solved and the passive force of the muscles in the deep flexor compartment was estimated. These results correspond well with the tibial traction theory, which suggests MTSS is caused by excessive traction to the tibial fascia at its insertion 2-8 cm above the medial malleolus. The results showed excessive foot pronation caused increased forces to be transmitted to passive elastic fibers of the deep flexor compartment (tibialis posterior, flexor digitorum longus and flexor halluces longus) [60].

Al Nazer et al. [61] constructed a generic lower body musculoskeletal model using BRG.LifeMODE 2007.0.0 in order to study the stresses and strains which develop MTSS. A computer model was built on the kinematics of a single subject, a healthy Caucasion man (25 years, height 184 cm, mass 89 kg) to study the tibial strains when walking. The subject was asked to perform a walking test on a level surface at constant speed. In order to track the human body motion, visual markers were placed on various locations of the subject. A motion capture system tracked segment trajectories during the walking performance. The trajectories were then used to drive the model in the inverse dynamics simulation where the desired muscles shortening/lengthening patterns were calculated [61]. The skeletal lower body model was generated from an anthropometric database. The multibody simulation approach with the floating frame of reference formulation was used to estimate tibial deformations during walking. In the floating frame of reference approach, large reference motions were described using a reference frame and the deformations of the tibia are described relative to the reference frame. This approach allows coupling of deformations and large reference motions in the inertia description of the tibia. The deformations of the tibia were described using the finite element approach. Due to the complex geometry of the tibia, the finite element model consisted of a large number of nodal degrees of freedom, which makes it computationally expensive to define the deformations in the time domain analyses. This computational problem was alleviated using the component mode synthesis. In the component mode synthesis, the deformations of the tibia were assumed to be linear with respect to the reference frame. The assumption made it possible to use modal coordinates instead of nodal coordinates in the description of tibial deformations. In this study, the modes denote vibration modes of the tibia obtained from an eigenvalue analysis of the tibial finite element model. The use of modal coordinates allowed a number of variables that describe

the deformation to be reduced. This, in turn, reduced the computational effort drastically without a significant loss of accuracy. The vibration modes were calculated by employing the Craig–Bampton method with the orthonormalization procedure. In the Craig–Bampton method, the vector of nodal coordinates of the finite element model was divided into boundary and interior nodal coordinates. The Craig–Bampton method results in two sets of modes, which are non-orthogonal constraint modes and orthogonal fixed interface normal modes. The constraint modes describe deformation due to unit displacements of boundary nodal coordinates, while the fixed interface normal modes describe vibration modes when fixed boundary conditions are applied at all the boundary nodal coordinates. The orthonormalization procedure was applied to the Craig–Bampton modes in order to enforce the deformation modes as orthogonal. In the finite element model of the tibia, nodes at the knee and ankle joints were selected as boundary nodal coordinates. The boundary nodes were connected via massless rigid beams to the nodes at the surface of the tibial metaphyses. The flexible tibia was used in forward dynamic analysis to calculate deformation due to dynamic loading. The strains during the walking exercises were obtained using the modal strain matrix that defines the relationship between the modal coordinates and strains of finite elements. The finite element model of the tibia was described in the ANSYS 8.1 software using shell elements. The thickness of each element was assumed to be equal to the average cortical wall thickness of the subject's tibial mid-shaft, which was 6.3mm as obtained from a peripheral quantitative computer tomographic (CT) scan. Young's modulus and the shear elastic modulus of the cortex bone were assumed to be 17 and 10 GPa, respectively, in the longitudinal direction along the bone, while they were assumed to be transversely isotropic with values of 5 and 3.5 GPa, respectively. The total number of nodal degrees of freedom of the

tibial finite element model was 61,872. The software ANSYS 8.1 was used to calculate the number of Craig–Bampton modes needed in the floating frame of reference formulation [61].

The methods used by Olesen et al., and Nazer et al., are similar in the regard to in silico experimentation. Both methods incorporate a single person's kinematic data with a 3-D model based on the research subject in order to perform the experimentation and analysis. However, Nazer *et al.* is a much more inclusive study, using multiple computational biomechanics programs. This method of determining stresses and strains in the musculoskeletal frame is what is needed to drive future biomechanics research.

Sheikh-Warak [95] conducted a study investigation explored how ground reaction forces together with the muscle forces required for different gaits (influenced by footwear) are transmitted onto the bones and joints in the lower limb. Specifically, the compressive, tensile and shear strains produced in the tibia throughout the running cycle for different running styles was investigated by developing an established musculoskeletal model and corresponding finite element model of the tibia [95]. The traditionally shod condition revealed the lowest tensile and compressive strains during initial contact with the ground due to the alignment of the tibia with the ground reaction force reducing its action in bending. Strains are larger on a small region at the distal end however due to muscle forces stabilizing the dorsiflexed foot at impact. The traditionally shod condition experiences greater strains overall - the medial tibial is strained 1.5 times higher on average. In addition it receives the largest strains overall during the maximum decelerating phase, "impact" phase of gait. Vertical ground reaction forces at this phase are 400 N higher on average [95].

Altman et al. [104] performed a similar study in which 5 subjects were utilized (2 men and 3 women) who ranged from 20 to 24 years old. All subjects were encouraged to run with a

rear-foot strike (heel strike) pattern. Each runner underwent a standard motion analysis data collection session. Shod rear-foot striking was collected during over-ground running at 3.5 m/s. Five trials were collected for each of the 3 conditions, and the trial which best represented the mean was used for analysis.

3D kinematics were calculated using inverse kinematics in Visual 3D (C-Motion, Rockville, MD), and exported into OpenSim (Simtk, Stanford, CA). Within OpenSim, the subject and segments were scaled according to the subject mass. Reduced residual analysis and computed muscle control were then used to calculate optimized kinematics and muscle forces used to drive the motion. Finally, the ankle joint contact force was calculated by combining the contributions from the ground reaction force and the muscle forces crossing the ankle joint [104].

A CT scan of the tibia of each subject's dominant lower limb was performed at Omega Imaging (Diagnostic Imaging Associates, Newark, DE). The tibia was extracted from the images using Mimics (Materialise, Leuven, Belgium) software to separate the bone from the surrounding tissues. A 3D mesh was generated using 8-node hexahedral elements [106].

Altman reported shear strains of 1.0E-09 to 3.0E-9 during the "impact" phase of gait. Shear strains that are also measured in this study. The peak tended to occur around 50% of stance, reflecting the point where the joint contact force is highest, or the "impact" phase of gait [104]. While peak strain can ultimately cause bone to fail at high magnitudes, it is also possible that the repeated high strain rates observed in running cause microfractures, which ultimately lead to stress fractures [105]. Altman expected the strain rate to be highest in the rearfoot strike condition due to the local maxima observed around the impact peak of the vertical ground reaction force. Sheikh-Warak reported that shod heel striking was found to produce compressive and tensile strains over 3000 microstrains for around 70% of the running cycle. The barefoot

condition was found to produce compressive and tensile strains over 3000 microstrains for the remaining 30%, with the minimally shod, mid-foot striking condition occupying a middle ground between the two. Shear strains above 5027 microstrains were extensive on the tibial plateau for the traditionally shod condition throughout most of the gait. Sheikh-Warak observed shear strain E12 in the mid-tibia to range from 3.49E-10 to 5.00E-9.

2.3 Use of Isotropic and Orthotropic Material Properties

Adaptation algorithms have been incorporated into finite element (FE) studies in many areas of biomechanics that focus on bone morphogenesis and response to altered loading conditions [63]. Bone was initially assumed to be a self-optimizing linearly elastic continuum that responded to changes in strain energy density (SED) [64-70]. Coelho *et al.* [71] and Kowalczyk [72] have used SED as the driving stimulus for the optimization of bone with a hierarchical macrostructural and microstructural description. However, SED can produce convergence problems during the adaptation process at a continuum level. The action of directional-dependent normal strains on the bone matrix has been put forward as the generator of physiological mechanobiological signals that activate osteocytes [73, 74] and better suited as the driving stimuli of the adaptation process in continuum models [68, 75, 76].

In order to model the process of bone adaptation, the driving stimulus needs to be a physiologically meaningful representation of the *in vivo* mechanical environment [63]. Therefore, the FE model of the bone developed by Geraldes et al. (2014) was required to be as close to the physiological state as is reasonably possible. This involved careful selection of its constitutive representation, mesh, geometry, loading and boundary conditions.

In order to simplify the analysis, 2D representations of the femur and partial models are commonly used and ignore the adaptation process in different planes or regions of importance.

Artificial boundary conditions, such as restricting displacement at a distal end of the femoral shaft, induce stress concentrations around the restrained region. Non-physiological loading conditions such as applying hip contact forces and muscle forces as point loads are often adopted for simplicity.

Bone is usually modelled with isotropic material properties in an attempt to reduce computational times [64, 65], despite the anisotropic nature of the material properties being measured experimentally [77-79]. Orthotropy has been shown to be the closest approximation to the bone's anisotropy, short of full anisotropic modelling [77]. In addition, isotropy is insufficient in predicting the directionality of the observed microstructure of the bone [80-83].

The need for a physiological continuum model of the material properties distribution and structure orientation across the femur in order to understand its biomechanical behavior has been emphasized [84]. A review of the regression equations that have been fitted between elastic properties measured experimentally and computed tomography (CT) derived densities suggests that it is difficult to accurately determine this relationship [63]. Furthermore, CT images are composed of scalar density values resulting from a combination of local porosity and tissue mineralization and, therefore, are not able to predict the directionally dependent elastic properties of the bone required to model its structural directionality at a continuum level [84]. Recent developments in micromechanics and X-ray physics [85] have allowed for extraction of orthotropic elastic properties from CT data. These studies rely on observer-dependent estimations of the trajectories of the principal material directions from the bone's geometry and from recognizable collagen structures amongst volumetric CT data of varying resolution [86-88].

A further advantage of using orthotropic material properties instead of isotropic symmetry is that directionality of the bone material properties can also be predicted. The

proposed continuum approach presented in this study circumvents the assumption of using a pre-defined library of microstructure geometry because it allows the system to optimize the combination of material orientations in order to provide the minimum energy solution for the load case it is subjected to [63].

Geraldes, D. M., & Phillips, A. [63] tentatively concluded that the orthotropic assumption is more advantageous in comparison with the isotropic material symmetry assumption. Orthotropy provides a more accurate representation of bone's elastic symmetry and can also give information about the three-dimensional directionality of bone's tissue-level material properties. The use of a balanced model allows for the prediction of the adaptation process for the whole femur, without artefacts induced by the application of fixed boundary conditions directly on the bone in question. An orthotropic model for the complete 3D femur has been produced. The inclusion of multiple load cases and of a shear modulus adaptation algorithm could further improve the predictions. A robust orthotropic continuum model of the whole femur has potential in achieving a more thorough understanding of bone's structural material properties, thus improving the knowledge we have of its mechanical behavior and response to the various loading environments it may be subjected to. Such a model could contribute to the improvement of the design of orthopedic implants and fracture fixation devices, providing information on the directional properties of the bone surrounding these devices and how it may adapt to the changing mechanical environment [63].

W.R. Taylor et al. [89] validated the use of FE bone models and establishing the distribution of orthotropic elastic constants throughout the bone. By comparing FE predictions of fundamental frequency with modal analysis results, this study has demonstrated a viable technique for both validating FE bone models and establishing the distribution of orthotropic

elastic constants throughout the bone. Comparison of mode shapes between the resulting FE model and the cadaveric bone displays a high level agreement and therefore demonstrates the quality of the results obtainable. The excellent agreement between the FE predicted density and major stiffness component and those determined for this bone using ultrasonic techniques show this approach to be viable for the determination of the distribution of elastic constants [89]. In reality, the high degree of anisotropy in cancellous bone can cause the ratios between the elastic moduli to be as high as 1:4 whereas ratios throughout this bone are approximately 1:1.7. This effect might be reduced if cancellous and cortical properties were to be defined separately [89].

Although this necessitates prior assumptions regarding the ratios of the elastic constants, which may vary from bone to bone, current understanding and findings suggest that the utilization of orthotropic material properties could yield useful results [89].

2.4 Finite Element Analysis

Finite element methods are widely used in biomechanics and bioengineering to solve ordinary and partial differential equations that represent physiological phenomena. In biomechanics, such phenomena include estimating stresses and strains in complicated mechanical systems. Finite element analysis (FEA) or finite element modelling (FEM) are generally synonymous terms for computer-based methods of stress analysis which are used when the shapes, numbers or types of materials, or the loading history are too complicated to yield to analytical methods [47].

Biomechanics studies often require parametric analysis or, the effects of changing various parameters in the model. Researchers are often content with modelling what could be described as an average or 'typical' system [47]. However, there are available statistical methods for designing experiments, called factorial designs, by which a large number of variables, each of

which can assume a range of values, can be analyzed much more efficiently than the common approach of varying one at a time while keeping the others fixed [48]. These have been used, e.g. by agronomists, for many decades and have found their way into engineering design in the automotive industry during the last two decades, due largely to the pioneering work of GenichiTaguchi [49].

Brekelmans, W. A. M. et al. [111] presented the first published study on the use of finite element methods on bone. The study demonstrated a mathematical model designed on the basis of the finite element method was to be preferred to existing techniques of studying the mechanical behavior of skeletal parts. Brittle coating and photo stressing techniques were used to map the structure of the human femur. A 2D model was created which then was extruded to a 3D model. By extruding from 2D to a 3D model, Brekelmans et al. could apply the anisotropic nature of bone.

Gray, H. A. et al. [112] created FE models of a human cadaveric tibia, both intact and implanted with a unicompartmental knee replacement, and validated the models against results obtained from a comprehensive set of experiments. Seventeen strain rosettes were attached to a human cadaveric tibia. Surface strains and displacements were measured under 17 loading conditions, which consisted of axial, torsional, and bending loads. The tibia was tested both before and after implantation of the knee replacement. FE models were created based on computed tomography (CT) scans of the cadaveric tibia. The models consisted of ten-node tetrahedral elements and used 600 material properties derived from the CT scans. The experiments were simulated on the models and the results compared to experimental results [112].

Donahue, T.L.H. et al [113] developed a geometrically accurate three-dimensional solid model of the knee joint with special attention given to the menisci and articular cartilage; determined to what extent bony deformations affect contact behavior; and determined whether constraining rotations other than flexion/extension affects the contact behavior of the joint during compressive loading. The model included both the cortical and trabecular bone of the femur and tibia, articular cartilage of the femoral condyles and tibial plateau, the transverse ligament, the anterior cruciate ligament, and the medial collateral ligament. The solid models for the menisci and articular cartilage were created from surface scans provided by a noncontacting, laser-based, three-dimensional coordinate digitizing system. Solid models of both the tibia and femur were created from CT images, except for the most proximal surface of the tibia and most distal surface of the femur which were created with the three-dimensional coordinate digitizing system [113].

Olesen, C. G. et al. [114] built a musculoskeletal model of the lower extremitiy in the AnyBody Modeling System. The model was based on cadaver data and included 38 muscles that were divided into 316 muscle fascicles, based on the line-of-action. A Hill-type muscle model with passive elasticity and force-length-velocity relationships was used. The model was driven through a gait cycle with kinematic and kinetic data from a gait experiment on a healthy male subject (173 cm; 85 kg). For simulating different degrees of pronation, the right foot was artificially rotated about an axis going from the calcaneus and through the 2nd metatarsal bone. The rotation went from 20˚ pronation to -5˚ supination, mimicking foot postures from highly pronated to slightly supinated. The simulations were run with increments of 5˚. For each foot posture the muscle recruitment problem was solved and the passive force of the muscles in the deep flexor compartment was estimated [114]

.

2.5 Factorial Design

Factorial design enables the estimation of the sensitivity of a system to variation in a large number of input parameters whilst reducing experimental effort. The Taguchi method lends itself well to FEA. The terminology used is familiar to engineers, and the methodology relies more on engineering judgment than absolute statistical values. In structural FEA, it is usually required to determine one or more response variables, such as maximum von Mises stress, minimum nodal displacement, etc. The many different material, geometrical, and loading parameters used as inputs for an FE model are called factors in Taguchi terminology. These are assigned discrete values, called levels, which divide equally the range of each factor [47].

New models employing the latest numerical methods in biomechanical analyses are being introduced at a fast pace. A feasible solution can be obtained by numerical optimization techniques when an empirically verified model is available and an objective is properly chosen. However, for some biomechanical studies incorporating many factors, such as a musculoskeletal system, the biomechanical analysis of human movement may become extremely complex. Hence the establishment of adequate and manageable models is very difficult in some studies [110]

The Taguchi's design of experiments (TDE), a highly fractional factorial design method, has been used extensively and successfully in many engineering fields. Recently Wang and Kong applied the TDE in solving an air bearing optimization problem. In the analysis, the experiments were replaced by solving an empirically verified numerical model, which is a highly nonlinear second-order partial differential equation. The TDE successfully predicted the global optimum settings for both two-level and three-level designs with four variables. Therefore, the potential use of TDE in biomechanical applications may be valid [110].

CHAPTER 3

Methodology

3.1 Creation of 3D Model

CT data of a human tibia was obtained from Fregly et al. [90] in a stereolithography file (.stl) format, and used as the basis for the geometry of the FEA model. The .stl file contains a wireframe geometry made from a series of polygons (triangular shapes) and typically used in visual software or for rapid prototyping. This .stl file was converted into an international graphics exchange file (.igs) using the Scan-to-3D add-in of the SolidWorks (x64 Student Edition) software. The .igs file was interpreted as a 3D solid by SolidWorks. 3D Solids are the best way to translate solid geometry to and from SolidWorks [107]. This is one of the formats that are the typical import/export method for bringing files into and out of SolidWorks successfully. The geometry contained is "dummy" geometry, which is an assigned geometry based on the CT data. It will not contain history, but it will have mathematically accurate solid geometry on import. The creation of the 3D solid model in SolidWorks allowed for the transition into finite element modeling.

From SolidWorks, the 3D model of the tibia is imported into Abaqus/CAE (6.13). This was done as an .igs file or by saving the 3D model as a "part" (.prt) file. In Abaqus, the material properties of cortical bone, isotropic and orthotropic, orientation, loading and boundary conditions can be applied to the model. Table 1 and Table 2 show the material properties used in the models.

3.2 Material properties

Bone has been previously modelled as an isotropic material, in an attempt to reduce computational cost [64, 65] [77-79], in spite of isotropy's insufficiency in predicting the

directionality of the observed microstructure of the bone [80-83]. Orthotropy has been shown to

be the closest approximation of the bone's behavior, short of full anisotropic modelling [77].

Recent developments in micromechanics and X-ray physics have allowed for extraction of

orthotropic elastic properties from CT data. Orthotropy provides a more accurate representation

of bone's elastic symmetry [80-83].The tibia model was assumed to be cortical bone with

orthogonal properties [89]. Microfractures in the tibia are more likely to be observed in the

cortical bone [104].

Table 1. Tibia Bone Material Properties [92]

Bone	Young's Modulus (Longitudinal, transverse)	Density	Poisson's Ratio	Tensile Strength	Compress. Strength	Failure Strength
Cortical	11-21 GPa	1.85 g/cm^3	0.46	60-70 MPa,~50MPa	70-280 Mpa, ~50MPa	0.01172 GPa
	5-13 GPa					
Cancellous	0.05-0.5 GPA	0.3-0.9g/cm^3		10-20 MPa	2-12 MPa	

Table 2. Orthotropic Material Properties of Tibia Cortical Bone [92]

Material Property	MPa
E1	6.91
E2	8.51
E3	18.4
G12	2.41
G13	3.56
G23	4.91
v12	0.49
v13	0.12
v23	0.14

3.3 Elements

After assigning material properties, a mesh was assigned to the model. The mesh divides up the 3D structure into elements. Elements may take the shape of hexahedrons, wedges, tetrahedrons, beam elements, or membrane elements. Hexahedral and tetrahedral elements are often considered the best choices when modeling bone [91]. Hexahedral elements are influenced less by the number of elements assigned and has a higher degree of stability than tetrahedral elements [91]. For the sake of this investigation a convergence study was performed to determine the best element shape and the number of elements needed. Convergence was achieved when the change in maximum von Mises stress, was less than 5%. The convergence study began with a minimum of 5,000 elements with an incremental increase of 500 elements. The final error level

for the converged model was 3.3%. During the convergence study, wedge elements did not reach an error of less than 5%. The tetrahedral element study stabilized but the number of elements required was too great for the limited memory of the academic license of Abaqus to process. The convergence study revealed that 39,874 hexahedral elements was computationally economical and had the least varying von Mises stress compared to tetrahedral and wedge elements. The elements have an edge length of 4.57 millimeters (mm) and an area of 15 mm^2.

3.4 Loading and Boundary Conditions

Tibia models were initially positioned at 0° about the y-axis in the "Assembly" module of Abaqus. Here, the model is rotated about the y-axis by 15° to the mid-sagittal plane of the body. Similarly, this same procedure is used to position the model 20° about the y-axis. The tibia was repositioned in this manner to simulate the action of standard pronation and over pronation. To mimic the different phases of gait, the bone was positioned according to the values of dorsiflexion and plantarflexion taken from the literature. A dorsiflexion angle of 24° was used to simulate the angle at which the heel of the foot would strike the ground. A plantarflexion of 41°, the angle of the tibia, was used to simulate the angle at which the foot is propelling forward, pushing off of the ground [26].
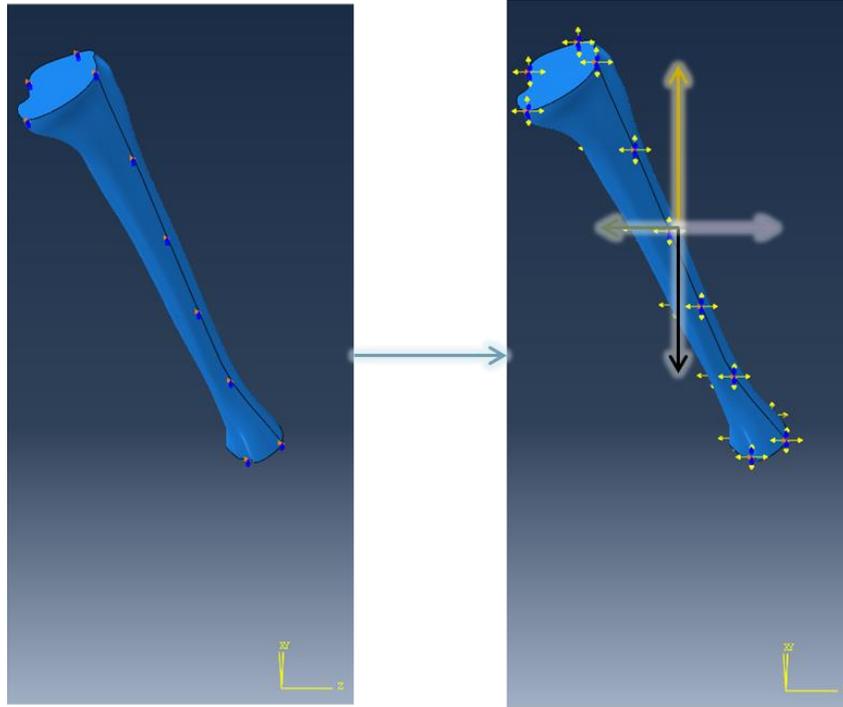
Figure 1. Loading and Boundary Conditions Application. The yellow arrows in the figure on the

right indicate and elimination of the degrees of freedom of the bone.

The 3D human tibia model in the "Assembly" module of Abaqus. In the "impact" phase of

running gait, this model has been rotated about the y-axis to simulate the action of pronation. The

yellow vector indicates the application of "ground reaction forces". The lavender vector is the

representation of "peak horizontal propulsion force". The black vector is the application of "body

force". The brown line represents the application of "peak horizontal breaking force". The

smaller yellow arrow vectors represent the same forces listed distributed along the edges of the

assembly.

Loading conditions included in this analysis consist of the "body force", "ground reaction

force", "propulsion force", and "peak breaking force" come from the literature Meardon, S. A.

[39]. Forces were input based on the subjects' body mass index (BMI) as a product of the

subjects' heights and masses. The 2 male subjects (1.78 m, 61.1 kg and 1.78 m, 79.5 kg) have a

normal BMI of 19.4 and a high BMI of 25.1. "Body forces" of 2391 N and 3116 N are considered to be directed towards the running surface. "Ground reaction forces" of 2010 N and 2490 N are considered to be forces directed upwards into the tibia. "Propulsion forces" of 309N and 440N are in the direction at which the athlete is running, and "peak breaking forces" of 200 N and 301 N [39] are forces directed in opposition to the direction of locomotion. These forces were inputted into the "Loading" module of Abaqus to apply the corresponding loads to models with normal and high BMI. The forces are assigned to the tibia model along the outermost element edges.

Isotropic and orthotropic models were run under simulations of both subjects having distinct body forces, ground reaction forces, propulsion forces, and peak breaking forces. The subjects' forces were measured for a velocity of 3.58 m/s (8 miles per hour) [95]. Von Mises stress, compressive stress, and shear strain in the X and Y directions (E12) were only recorded for the medial tibial region. Stresses and strains experienced on the lateral, anterior, and posterior tibia were not reported.

All simulations were run in Abaqus under quasistatic conditions. Time and inertial mass were not considered in this analysis as it was the initial pass at generating these models [108]. Von Mises stress is widely used in various industries that employ the finite element method. The concept of Von mises stress is thought of as an equivalent stress and is based arises from the distortion energy failure theory and octahedral stress calculations. Distortion energy failure theory is comparison between 2 kinds of energies, 1) Distortion energy in the actual case 2) Distortion energy in a simple tension case at the time of failure. According to this theory, failure occurs when the distortion energy in actual case is more than the distortion energy in a simple tension case at the time of failure [93].

3.5 Statistical Analysis

Factorial analysis of variance (ANOVA) measures the probability of a combination of independent variables predicting the value of a dependent variable. This particular analysis was used to determine interactions between the independent variables or factors considered. An interaction implies that differences in one of the factors depend on differences in another factor [47]. The independent factors being investigated in this study are level of pronation (15° and 20°) and body mass index with 2 varying quantifiable levels (19.4 and 25.1). This study also investigates the possibility of gait phase has an independent factor with 3 varying categorical levels (impact, mid-stance, and push-off) and material property with 2 varying levels (isotropic and orthotropic). The independent factors were tested in order to determine whether there was any interaction between risk factors in developing high von Mises stress, compressive stress, and shear strain.

3.6 Validation

Validation for this study was done by comparing results from this study to existing literature. Burr et al. (1996) hypothesized that strains >3000 microstrain could be produced on the human tibial mid-shaft during vigorous activity. Strains were measured on the tibia of two subjects via implanted strain gauges under conditions similar to those experienced by Israeli infantry recruits. Principal compressive and shear strains were greatest for uphill and downhill zigzag running, reaching nearly 2000 microstrain in some cases, about three times higher than recorded during walking. Burr et al.'s results showed that strain is maintained between 1444 to 1966 microstrains in the medial tibia when subjects ran on a level surface [115].

CHAPTER 4

Results

4.1 Isotropic Results

All tibia models in this section were assigned isotropic material properties. The models were run under simulations of 2 male subjects having different body forces, ground reaction forces, propulsion forces, and peak breaking forces. The subjects' forces were measured for a velocity of 3.58 m/s (8 miles per hour). Von Mises stress, compressive stress, and shear strain E12 were only recorded for the medial tibial region. Stresses and strains experienced on the lateral, anterior, and posterior tibia were not recorded.

Four models were tested for the 3 main phases of running gait for a total of 12 models with orthotropic material properties. These models were run with the following corresponding boundary conditions: pronation 15° and BMI 19.4, pronation 15° and BMI 25.1, pronation 20° and BMI 19.4, and pronation 20° and BMI 25.1. By running these models as a factorial design, it was believed that a correlation between risk factors causing greater stress and strains would be determined.

4.1.1 Impact Phase of the Gait Cycle
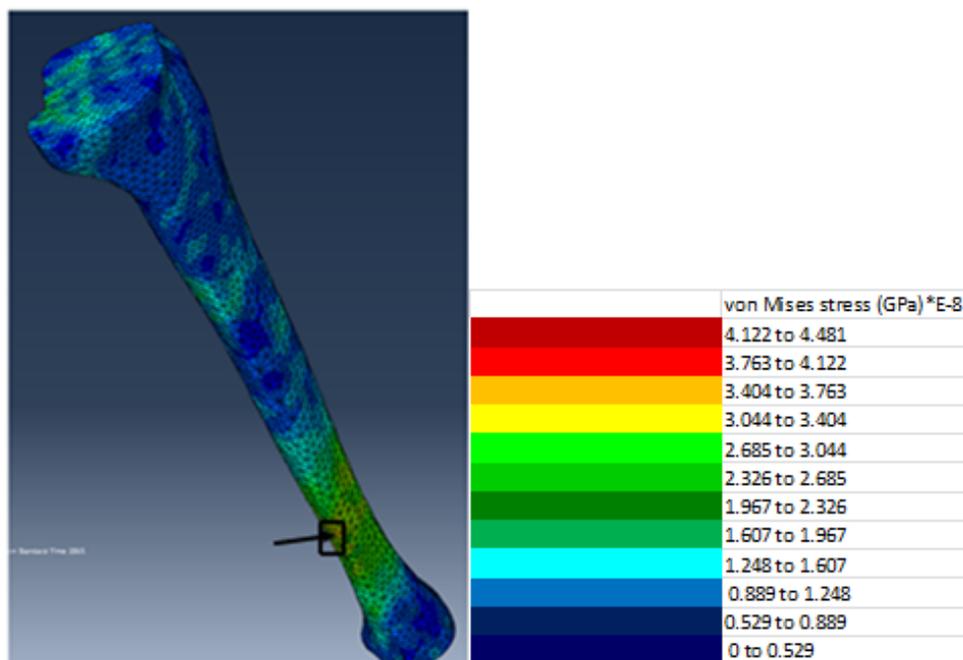
Figure 2 Isotropic Impact Model

Figure 2 is an isotropic model with boundary conditions of over pronation at 20° and a high BMI of 25.1. The subject is striking the ground with a dorsiflexion of 24°. The combination of over pronation and high BMI in this model produced the highest von Mises stress out of all isotropic tibia models in the impact phase of gait. A maximum von Mises stress of 3.46E-8 GPa was recorded in the distal medial tibia indicated by the black arrow and box.

4.1.2 Mid-stance Phase of the Gait Cycle

von Mises stress (GPa)*E-8
3.079 to 3.359
2.799 to 3.079
2.519 to 2.799
2.239 to 2.519
1.959 to 2.239
1.679 to 1.959
1.4 to 1.679
1.12 to 1.4
0.84 to 1.12
0.56 to 0.84
0.28 to 0.56
0 to 0.28
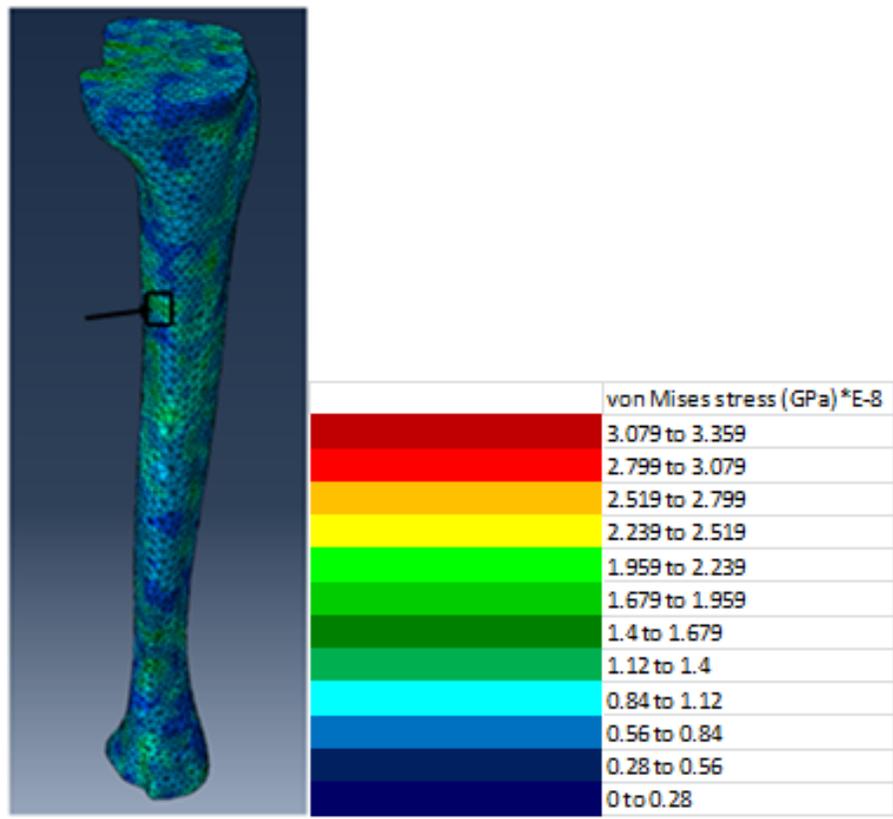
Figure 3 Isotropic Mid-stance Model.

Figure 3 is a model with isotropic properties with a pronation of 20° and BMI of 25.1. This model with a combination of the high levels for both risk factors produced the highest von Mises stress compared to the 3 other models run for this gait phase. A von Mises stress of 1.73E-8 GPa was recorded in the medial tibia towards the posterior face.

4.1.3 Push-off Phase of the Gait Cycle
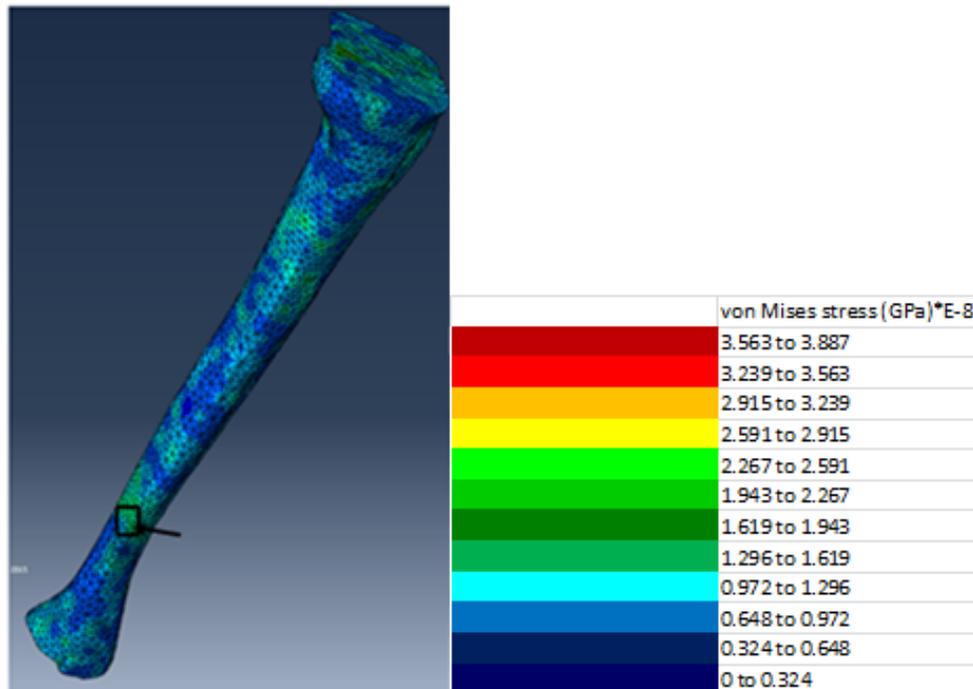
Figure 4 Isotropic Push-off Model.

Figure 4 is an isotropic model in the push-off phase of gait with over pronation and high BMI. This combination model produced the highest von Mises stress out of all isotropic tibia models in the push-off phase of gait. A maximum von Mises stress of 1.84E-8 GPa was recorded in the distal medial tibia.

4.1.4 All Isotropic Model Results

It was observed that the "impact" phase of gait produced the greatest stress and strain. Impact models with an increased level of pronation had the highest von Mises stress and compressive stress, 3.46E-8 GPa von Mises stress and 3.83E-8 GPa compressive stress. However, an impact model with a normal degree of pronation and high BMI yielded the greatest shear strain 2.47E-9. At this point, a high degree of pronation and high BMI yield the greatest

stress, but pronation may not have as much of an effect on strain. Stress and strain may vary between different phases of gait.

Table 3. Isotropic Model Maximum Stresses andStrain

Gait Phase	Pronation°	BMI	von Mises stress (Gpa)	Stress (Gpa)	Shear Strain, E12
Impact	15	19.4	1.49E-08	1.89E-08	1.70E-09
Impact	15	25.1	2.14E-08	2.75E-08	**2.47E-09**
Midstance	15	19.4	1.56E-08	1.88E-08	9.57E-11
Midstance	15	25.1	1.84E-08	2.31E-08	1.38E-10
Pushoff	15	19.4	1.07E-08	1.68E-08	9.49E-10
Pushoff	15	25.1	1.72E-08	2.10E-08	9.78E-10
Impact	20	19.4	2.95E-08	3.20E-08	1.00E-09
Impact	20	25.1	**3.46E-08**	**3.83E-08**	1.31E-09
Midstance	20	19.4	1.35E-08	1.49E-08	5.05E-10
Midstance	20	25.1	1.73E-08	1.88E-08	2.19E-10
Pushoff	20	19.4	1.59E-08	1.95E-08	1.76E-09
Pushoff	20	25.1	1.84E-08	2.05E-08	7.65E-10

4.2 Orthotropic Results

All tibia models in this section were assigned orthotropic material properties. The models were run under simulations of 2 male subjects having different body forces, ground reaction forces, propulsion forces, and peak breaking forces. The subjects' forces were measured for a velocity of 3.58 m/s (8 miles per hour). Von Mises stress, compressive stress, and shear strain

E12 were only recorded for the medial tibial region. Stresses and strains experienced on the lateral, anterior, and posterior tibia were not recorded.

Four models were tested for the 3 main phases of running gait for a total of 12 models with orthotropic material properties. These models were run with the following corresponding boundary conditions: pronation 15° and BMI 19.4, pronation 15° and BMI 25.1, pronation 20° and BMI 19.4, and pronation 20 ^{o} and BMI 25.1. By running these models as a factorial design, it was believed that a correlation between risk factors causing greater stress and strains would be determined.

4.2.1 Impact Phase of the Gait Cycle

	von Mises stress (GPa)*E-8
	5.383 to 5.872
	4.894 to 5.383
	4.404 to 4.894
	3.915 to 4.404
	3.425 to 3.915
	2.936 to 3.425
	2.447 to 2.936
	1.957 to 2.447
	1.468 to 1.957
	0.979 to 1.468
	0.489 to 0.979
	0 to 0.489
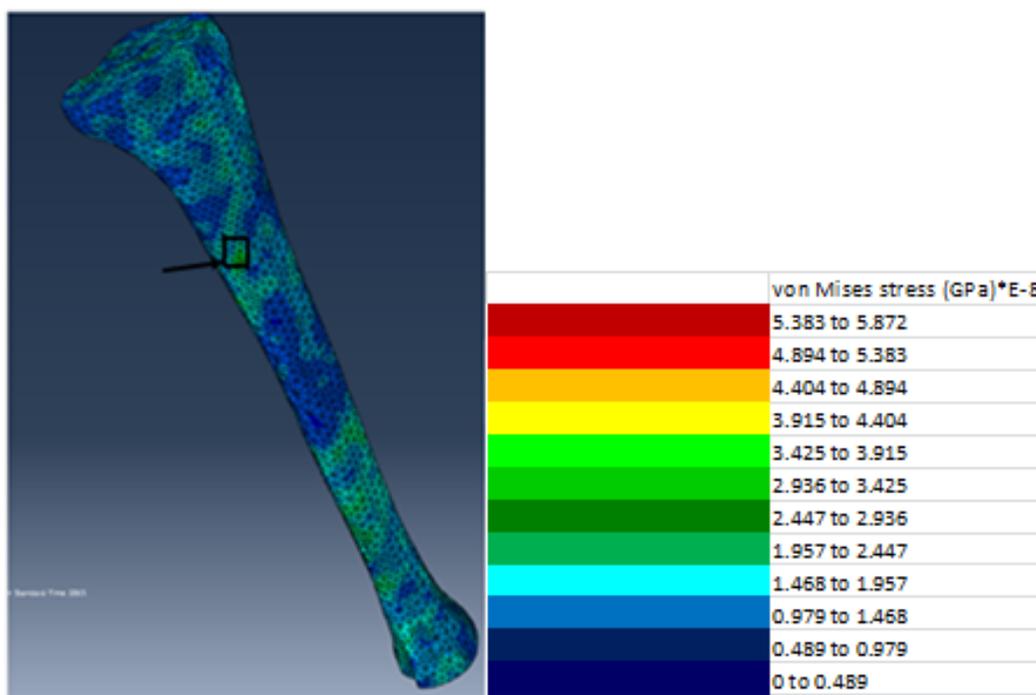
Figure 5 Orthotropic Impact Model.

Figure 5 is an orthotropic model in the impact phase of gait with over pronation and high BMI. This combination model produced the highest von Mises stress out of all isotropic tibia

models in the impact phase of gait. A von Mises stress of 2.28E-8 GPa was recorded in the medial tibia.

4.2.2 Mid-stance Phase of the Gait Cycle

von Mises stress (GPa)*E-8
6.72 to 7.30
6.142 to 6.72
5.563 to 6.142
4.984 to 5.563
4.406 to 4.984
3.827 to 4.406
3.249 to 3.827
2.67 to 3.249
2.091 to 2.67
1.513 to 2.091
0.934 to 1.513
0 to 0.934
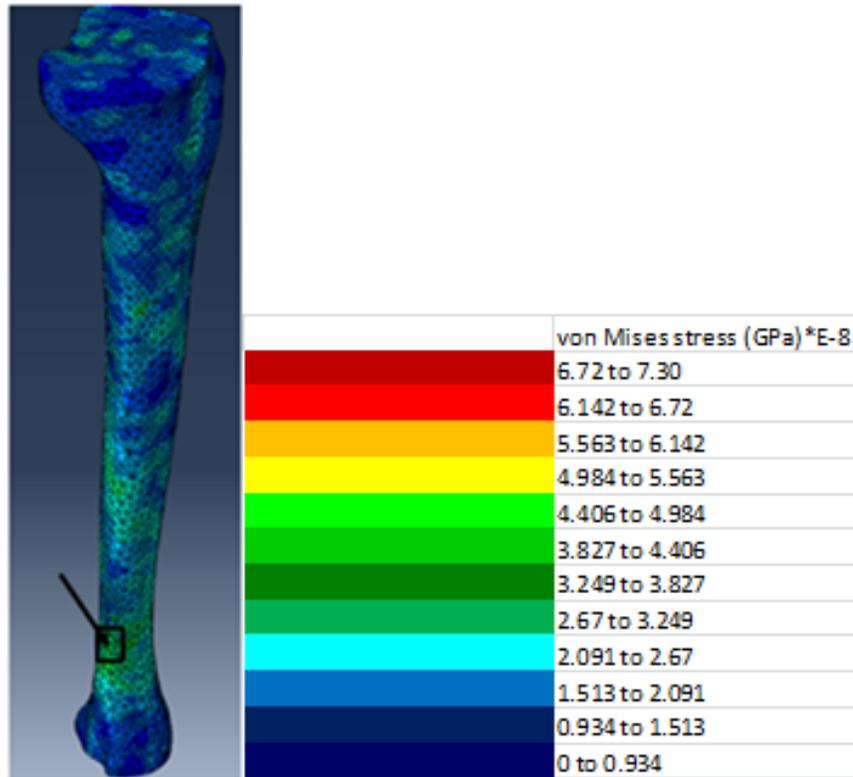
Figure 6 Orthotropic Mid-stance Model.

Figure 6 is an orthotropic model in the mid-stance gait phase with over pronation and high BMI. This model reported the highest von Mises stress of all orthotropic models in this gait phase. A von Mises stress of 3.50E-8 GPa is seen in the distal medial tibia.

4.2.3 Push-off Phase of the Gait Cycle
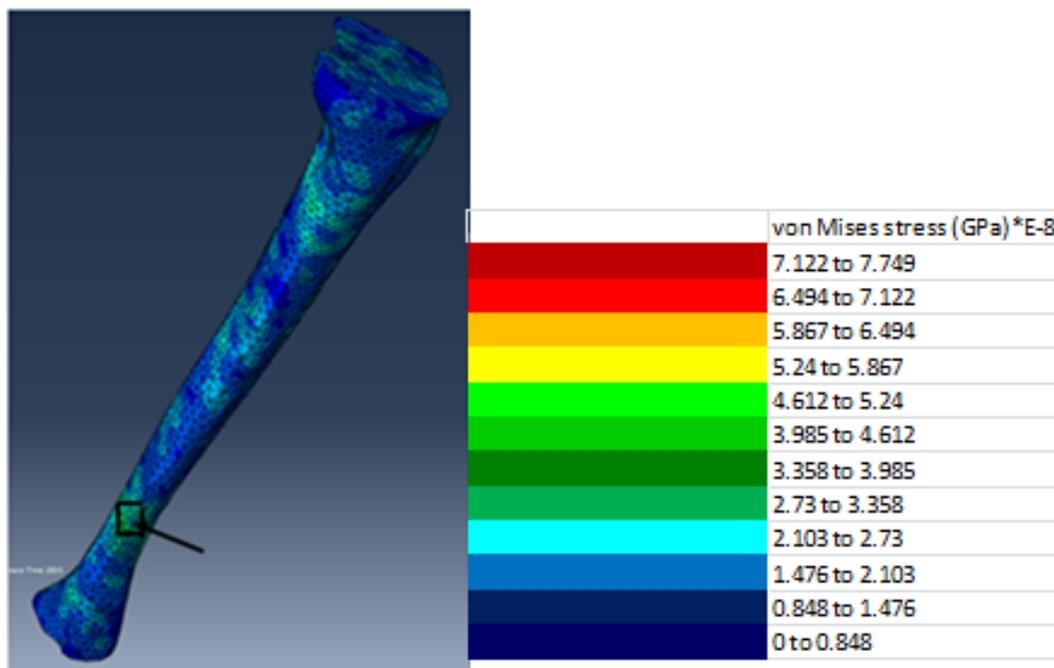
Figure 7 Orthotropic Push-off Model.

Figure 7 is an orthotropic model in the push-off gait phase with over pronation and high

BMI. This model under the conditions yielded the highest von Mises stress of all orthotropic

models in the gait phase. A von Mises stress of 3.64E-8 GPa is seen originating in the distal

medial tibia.

4.2.4 All Orthtropic Model Results

Orthotropic models had the highest von Mises stress and compressive stress results in the

"push-off" and "mid-stance" phases of gait. This varies when compared with the isotropic model

results. A maximum von Mises stress of 5.16E-8 GPa was observed for the "push-off" model

with a high level of pronation and normal level of BMI. A maximum compressive stress of

5.48E-8 GPa was observed for the "mid-stance" model with high pronation and normal BMI.

The maximum shear strain 2.23E-9 occurred once again for the "impact" gait phase with normal

pronation and high BMI. At this point, there may be an association with pronation and stress whereas BMI may have more of an effect on shear strain.

Table 4. Orthotropic Model Maximum Stresses and Strain

Gait Phase	Pronation°	BMI	von Mises stress (Gpa)	Stress (Gpa)	Shear Strain, E12
Impact	15	19.4	2.43E-08	3.25E-08	1.56E-09
Impact	15	25.1	2.70E-08	4.97E-08	**2.23E-09**
Midstance	15	19.4	2.37E-08	3.03E-08	1.82E-09
Midstance	15	25.1	2.65E-08	2.69E-08	1.84E-09
Pushoff	15	19.4	3.54E-08	3.81E-08	2.08E-09
Pushoff	15	25.1	3.17E-08	3.66E-08	1.75E-09
Impact	20	19.4	1.66E-08	1.81E-08	1.15E-09
Impact	20	25.1	2.28E-08	2.49E-08	1.68E-09
Midstance	20	19.4	3.95E-08	**5.48E-08**	2.03E-09
Midstance	20	25.1	3.50E-08	4.92E-08	2.37E-09
Pushoff	20	19.4	**5.16E-08**	3.09E-08	1.07E-09
Pushoff	20	25.1	3.64E-08	3.96E-08	1.46E-09

4.3 Statistical Analysis

Statistical results were obtained using Minitab 17 (Academic License, Minitab, Inc., State College, PA). A factorial ANOVA was performed to evaluate the impact of the risk factors produced by the varying levels of gait phase, pronation degree, BMI, and material property. From Table 5 there is a low P-value for pronation degree with a $P=0.048$. This low P-value means that pronation degree has a significant effect on the von Mises stress produced in isotropic

and orthotropic models. Gait phase with a P=0.648 and BMI with a P=0.995 do not appear to have much effect on the von Mises stress produced when using Nested ANOVA.

Table 5. Factorial ANOVA: von Mises stress versus Gait Phase, Pronation Degree, BMI, material

Factorial ANOVA for von Mises stress (Gpa*E-8)

Source	DF	Adj SS	Adj MS	F-Value	P-Value
Gait Phase	2	0.6075	0.3038	0.503	0.648
Pronation Degree	3	1.8102	0.6034	3.541	**0.048**
BMI	6	1.0224	0.1704	0.103	0.995
material	12	19.8332	1.6528		
Total	23	23.2734			

A factorial ANOVA was run to determine the significance that pronation degree, BMI, and gait phase had on the compressive stress yielded by isotropic and orthotropic models. Table 6 shows pronation degree with a P=0.024. This low P-value provides the researcher with the knowledge that pronation degree has a significant effect on the compressive stress yielded by all models. However, similar to the Nested ANOVA, this table reveals that BMI and gait phase have less significant effects on von Mises stress with respective P-values of P=0.667 and P=0.561.

Table 6. Factorial ANOVA: Compressive Stress versus Pronation Degree, BMI, Gait Phase

Factorial Analysis of Variance for Compressive Stress (Gpa*E-8)

Source	DF	Adj SS	Adj MS	F-Value	P-Value
Pronation Degree	1	1.730	1.730	1.58	**0.024**
BMI	1	0.099	0.099	0.09	0.667
Gait Phase	2	0.608	0.304	0.28	0.561
Error	19	20.837	1.097		
Total	23	23.273			

What is interpreted from Table 7 is that material property and BMI had significant effects on shear strain E12 with respective P-values of P=0.031 and P=0.027. Contrary to the factorial ANOVA for von Mises stress and compressive stress, pronation did not have a significant effect on shear strain.

Table 7. Factorial ANOVA Shear Strain E12 vs Pronation Degree, BMI, Material Property

Analysis of Variance

Source

	DF	Adj SS	Adj MS	F-Value	P-Value
Pronation Degree	1	1.7305	1.73046	2.68	0.664
BMI	1	0.0989	0.09891	0.15	**0.027**
Material Property	1	8.5332	8.53323	13.22	**0.031**
Error	20	2.9108	0.64554		
Total	23	23.2734			
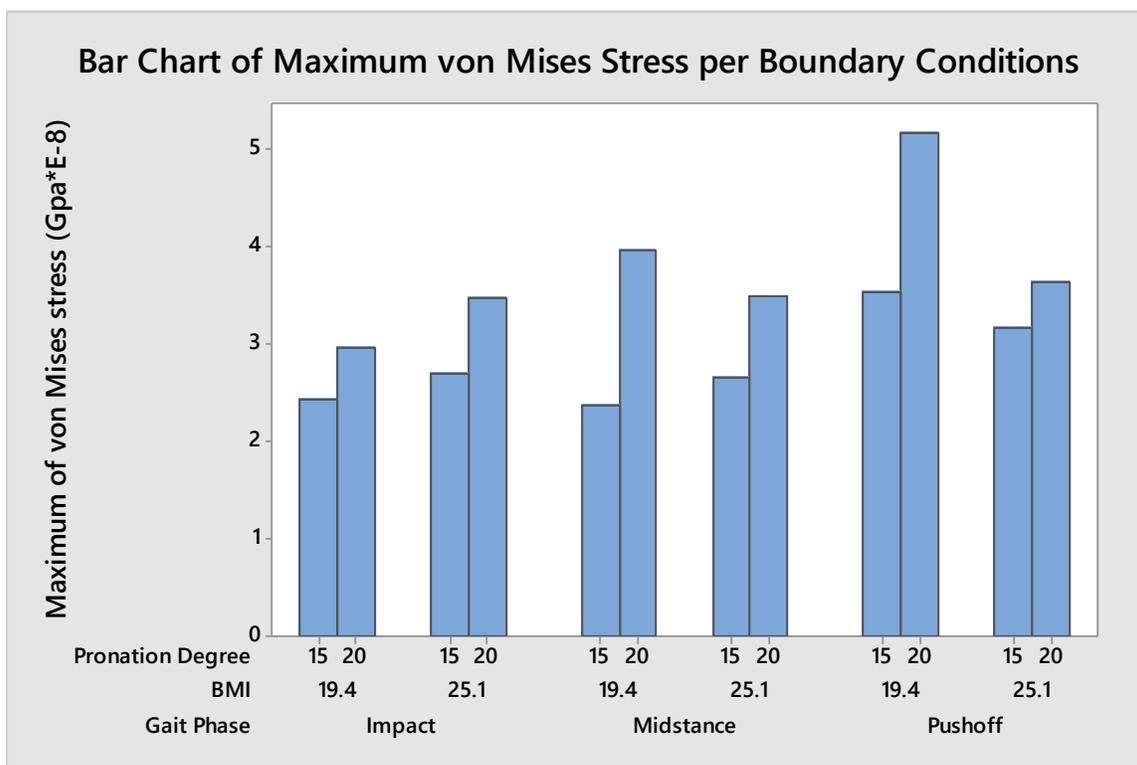
Figure 8 Maximum von Mises Stress for each degree of pronation, for each level of BMI, during

each of the Gait Phases.

Figure 8 is a bar chart of the maximum von Mises stress reported for each degree of

pronation and level of BMI for the three phases of gait studied. It was observed that a higher

degree of pronation increased the von Mises stress experienced by a tibia. Body mass index did

not necessarily increase the von Mises stress. An increased degree of pronation increased von

Mises stress for each phase of gait. Von Mises stress was greatest in the "Push-off" phase of gait.
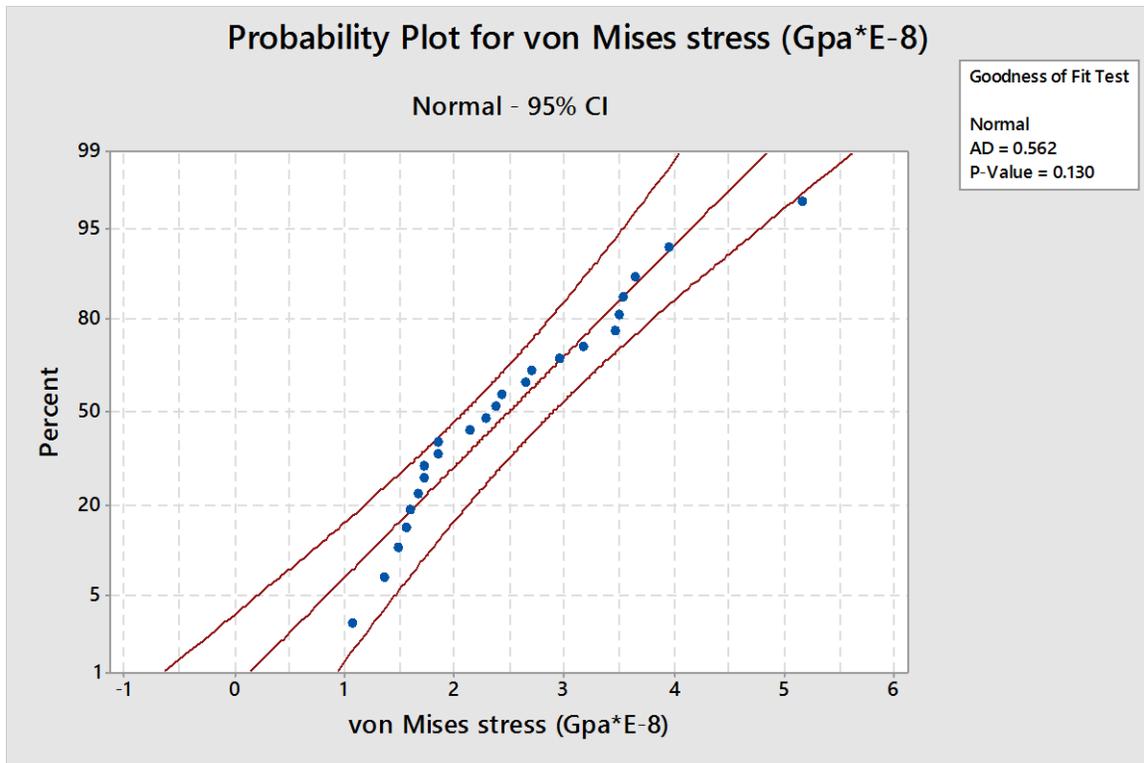
Figure 9 Normality Test for von Mises stress to determine statistical outliers,This graph shows a

possible outlier in the distribution but with a P=0.130, it did not change the statistical

significance.

The probability plots above test for normality. A given distribution is a good fit if the

data points roughly follow a straight line. The p-value is greater than 0.05. In this case, the von

Mises stress data appear to follow a normal distribution. The distribution represents the range of

maximum von Mises stress reported for all models. Because P=0.130 and there is a 95%

confidence interval, there are no statistical outliers. If a value were statistically significant, it

would fall outside of this confidence interval.
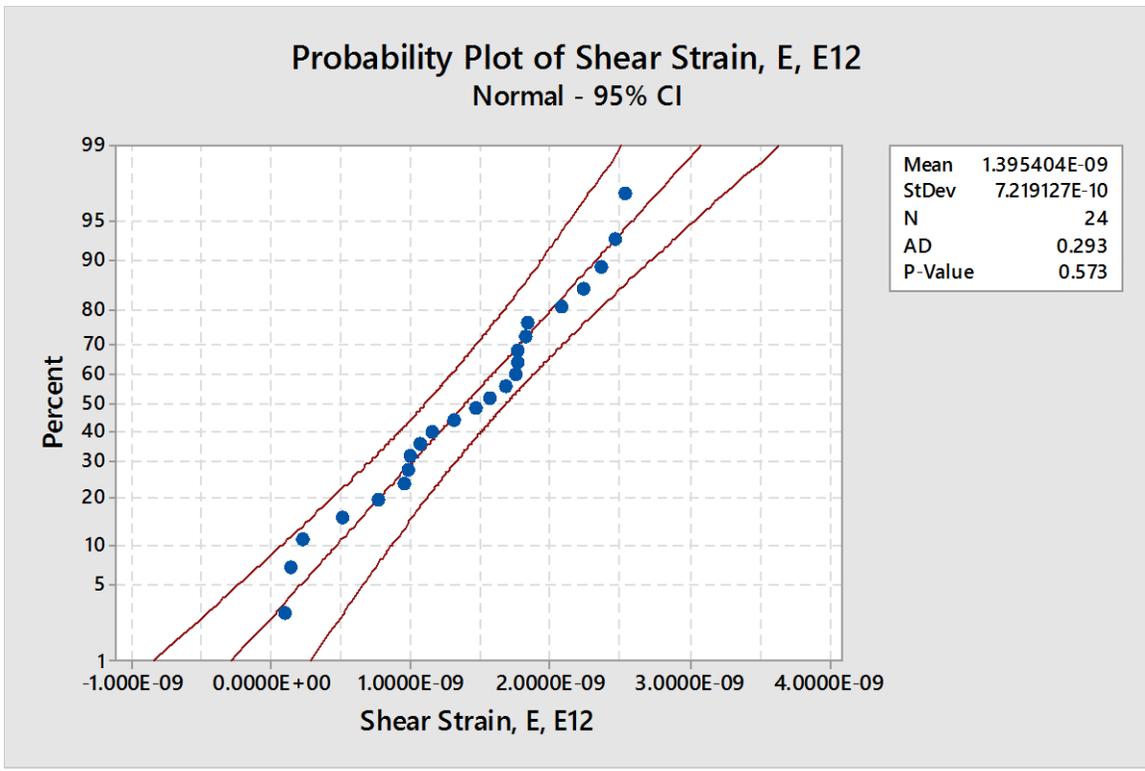
Figure 10 Normality Test for Shear Strain to determine statistical outliers

The probability plot above tests for the normality of shear strains recorded. No measurements fall outside of the 95% confidence interval. It can be assumed then that all shear strains were within an acceptable range. The shear strain reported for all models follows a normal distribution with a P-value of P=0.573. All shear strain results fall within the 95% confidence interval; therefore there are no statistically significant differences reported for the shear strain.

CHAPTER 5

Discussion and Future Research

5.1 Model Results

The purpose of this research is to model a human tibia under conditions that produce high stress and strains. This is important to study because such high stresses and strains could lead to microfractures and the development of MTSS. It was hypothesized that a combination of over pronation and high body mass index would yield a high stress and strain in the medial tibial region. A second hypothesis is that modeling the bone as an orthotropic material will yield higher stresses and or strains in the medial tibia region than models with isotropic material properties. To accomplish this, the risk factors of pronation and body mass index were used within normal and high or maximum levels.

Models with isotropic properties had a lower von Mises stress on average compared to models with orthotropic properties. The cause of this could be that orthotropic properties more closely associate with the structure of bone when compared to isotropic properties [89]. An additional advantage of using orthotropic material properties instead of isotropic symmetry is that directionality of the bone material properties can also be predicted. The proposed continuum approach presented in this study circumvents the assumption of using a pre-defined library of microstructure geometry because it allows the system to optimize the combination of material orientations in order to provide the minimum energy solution for the load case it is subjected to [63]. Geraldes et al. [63] tentatively concluded that the orthotropic assumption is more advantageous in comparison with the isotropic material symmetry assumption. Orthotropy provides a more accurate representation of bone's elastic symmetry and can also give

information about the three-dimensional directionality of bone's tissue-level material properties [63].

In addition to the effect material properties had on the von Mises stress, increased pronation and body mass index did increase the average von Mises stress experienced by each model in all phases of gait. The combination of over pronation and increased BMI supports the first hypothesis that the junction of these risk factors would most likely cause a stress great enough to produce microfractures causing MTSS [104]. When researching the effects risk factors have for von Mises stress, pronation had the highest significant effect. Excessive pronation induces an increased compensatory internal rotation of the tibia that results in overloading stress [105]. In this study, it was observed that excessive pronation of the tibia leads to overloading stress and strain.

The compressive stresses, similar to the von Mises stresses, were within an acceptable range across all models. On average, orthotropic models experienced greater compressive stresses than isotropic models. The combination of over pronation and increased BMI also produced greater compressive stresses on average compared to models that had normal pronation and normal BMI. Pronation had the highest significant effect on compressive stress. For both von Mises stress and compressive stress, the "push-off" gait phase increased the likelihood of microfractures, compared to the "impact" and "mid-stance" phases which decreased the stress experienced by the tibia. The first and second hypotheses are supported again by the compressive stress results.

The shear strain E12 was within an acceptable range across all models according to the normality test. On average, models with orthotropic material properties experienced greater shear strain than models with isotropic material properties. This supports the second hypothesis that

models with orthotropic material properties would experience greater shear strain than those with isotropic material properties. Unlike the statistical results yielded for von Mises stress and compressive stress; from Table 7, it is observed that material property and BMI have the most significant effects on shear strain, followed by pronation degree and gait phase in decreasing level of significance. Sheikh-Warak, compared the strains in the tibia under running conditions of differently, shod shoes. Sheikh-Warak reported shear strains of 3.49E-10 to 5.00E-09 between the distal and medial tibia [95]. The shear strains reported for orthotropic material properties in this study ranged from 1.07E-09 to 2.53E-09, which fits this range of strains Warak reported. Sheikh-Warak's work is physically validated by morphological data collected by Horsman et al. [109] and Burr et al. [115]. The "impact" phase of gait increased the shear strain experienced by the tibia. Sheikh-Warak also noted that the greatest shear strain was experienced during the maximum deceleration phase or "impact" phase [95]. This also supports the shear strain results yielded by gait phase in the study. Burr et al. reported 1444 to 1966 microstrains. The results of this study correlate to what Sheikh-Warak and Burr reported.

By examining the difference in von Mises stress, compressive stress, and shear strain across the phases of gait, it should be considered that either the stress experienced by the "push-off" or the strain experienced by the "impact" is what initiates the microfractures in the cortical tibia bone. Due to the limit of this study being that these models are under a one-time application of loads, it cannot be concluded that one phase or the other is responsible. Because MTSS is a repetitive stress injury, the simulations would have to be run thousands of times in order produce more useful results. However, this may allow researchers to ignore the "mid-stance" phase as having any significance in the development of MTSS. More studies are needed to verify the von Mises stress and compressive stress results found in this study.

5.2 Limitations

The results of this study are limited because the models were run under the assumption of an entirely cortical bone. Time permitting, a human musculoskeletal model of the lower extremity composed of cortical and cancellous bone of orthotropic and anisotropic properties may have yielded more accurate results. While this study provided knowledge on the phases of gait that cause the greatest stresses and strains, it has limitations. There was no physical validation test performed for this study. A cadaveric study of the lower extremity under running simulation would have provided useful data to compare the results found in this study.

A limitation of these studies in simulating the stress and strain effects that are experienced by the tibia is when a subject runs on an incline or decline surface. Many studies do not address this limitation [97], but this risk factor of running surface angle has been associated with MTSS. Other factors such as Q-angle, level of shod in the running shoe, age, joint kinematics, wind resistance [98], stride length, and range of motion [29] are difficult to model in finite element analysis due to what is computationally possible. Only male subjects were considered, but there have been studies performed solely on female athletes [42].

Every tibia model was assumed to be one solid piece of orthogonal cortical bone. A model with cancellous anisotropic bone as well as muscle tissue would contribute to a model of greater accuracy. However, due to the limitation of the Abaqus/CAE (6.13 student edition) these added features would not have been computationally economical. When modelling this orthogonal bone, a quasistatic linear elastic analysis was performed. A model using a dynamic non-linear viscoelastic analysis would provide a more accurate simulation of a tibia bone when running.

5.3 Future Research

Future studies should include physical validation by developing a 3D print of a tibia bone and comparing physical simulation to a cadaveric bone. When creating finite element models, in order to narrow the risk factors of MTSS skeletal models are needed as well as musculoskeletal models in order to test a wider variety of risk factors. The pathophysiology of medial tibial stress syndrome remains controversial. Some authors suggest an inflammation of the periosteum due to excessive traction (traction theory) [99]; others support the view that MTSS is not an inflammatory process of the periosteum, but rather a bone stress reaction (bone stress theory) as in stress fractures [100]. Although that MTSS and stress fractures constitute different pathologies [101], they sometimes coexist and it is likely that MTSS and stress fractures of the tibia are invoked by similar mechanisms, where MTSS is a relatively mild expression and stress fracture is a severe extreme [102]. The coincidence of the most common site of tibial stress fracture at or near the junction of the middle and distal thirds with the site of incidence of MTSS bolsters this suspicion [103].

Anatomical muscular skeletal models created by the CT scan data collected by a number of subjects could have all known tissue material properties assigned to each model. Kinematic and force data could be collected from recording movements and forces by a subject running across differently angled surfaces, wearing athletic shoes of varying levels of shod, varying velocities, differently gendered, and a wide age range.

Further research is needed to narrow the field of risk factors associated with MTSS. For this study, it was concluded that when examining the stress experienced by a tibia while running, pronation has a significant effect. However, when examining strain, body mass index had a more significant effect than pronation. An unexpected result of this study found that the "push-off"

gait phase produced the greatest von Mises and compressive stresses, whereas the "impact" gait phase produced the greatest shear strain.

In regards to which risk factor is most influential, degree of pronation seemed to cause a significant change in two of the outcome variable, von Mises stress and compressive stress. Despite the name of the term, medial tibial stress syndrome may be caused by the shear strain exerted on the tibia just as much as the stress. A more accurate bone model with cancellous bone and anisotropic properties may yield more accurate results. In the case of the effects that pronation and body mass index have on the stress and shear strain of the tibia cortical bone, it may be safe to conclude that the combination of these risk factors are more likely to cause microfractures developing leading to MTSS.

References

1. Slocum DB. The shin splint syndrome. Medical aspects and differential diagnosis. Am J Surg 1967; 114(6):875-881.

2. Moen, M. H., Tol, J. L., Weir, A., Steunebrink, M., & De Winter, T. C. (2009). Medial tibial stress syndrome. Sports medicine, 39(7), 523-546.

3. Beck, B. (1998). Tibial stress injuries. an aetiological review for the purposes of guiding management. Sports Medicine, 26(4), 265-279.

4. Fulgham, K. (2012). Medial tibial stress syndrome (shin splints). Unpublished manuscript, Retrieved from http://www.ghsa.net/medial-tibial-stress-syndrome-shin-splints

5. Magnusson HI, Ahlborg HG, Karlsson C, et. al. Low regional tibial bone density in athletes with medial tibial stress syndrome normalizes after recovery from symptoms. Am J Sports Med 31(4): 596-600, 2003

6. Kirby, K. (2010). Current concepts in treating medial tibial stress syndrome. Podiatry Today, 23(4), 52-57. Retrieved from http://www.podiatrytoday.com/current-concepts-in-treating-medial-tibial-stress-syndrome

7. Rompe, J. D., Cacchio, A., Furia, J. P., & Maffulli, N. (2010). Low-energy extracorporeal shock wave therapy as a treatment for medial tibial stress syndrome. The American journal of sports medicine, 38(1), 125-132.

8. Gaeta, M., Mileto, A., Ascenti, G., Bernava, G., Murabito, A., & Minutoli, F. (2013). Bone stress injuries of the leg in athletes. La radiologia medica, 118(6), 1034-1044.Bouche RT, et al. J Am Podiatr Med Assoc 2007 Jan; 97(1): 31-6.

9.	Gore, R., Mallory, R., & Sullenberger, L. (2008). Bilateral lower extremity compartment syndrome and anterior tibial stress fractures following an army physical fitness test. The Medscape Journal of Medicine,10(4), 82.

10.	Winters, M., Veldt, H., Bakker, E., & Moen, M. (2013). Intrinsic factors associated with medial tibial stress syndrome in athletes: A large case-control study.South African Journal of Sports Medicine, 25(3), 63-67.

11.	Moen MH, Bongers T, Bakker EW, Zimmermann WO, Weir A, Tol JL, Backx FJG. Risk factors and prognostic indicators for medial tibial stress syndrome. Scand J Med Sci Sports 2012;22:34-9.

12.	Hubbard, T., Carpenter, E, & Cordova, M. 2009, "Contributing factors to medial tibial stress syndrome: a prospective investigation", Medicine and Science in Sport and Exercise, Vol. 41, No. 3, pp. 490 – 496.

13.	Nigg, B. M. (2001). The role of impact forces and foot pronation: a new paradigm. Clinical journal of sport medicine, 11(1), 2-9.

14.	Hintermann, B., & Nigg, B. M. (1998). Pronation in runners. Sports Medicine, 26(3), 169-176.

15.	Couture D.J, Karlson K.A. Tibial stress injuries: decisive diagnosis and treatment of "shin splints." Physician Sportsmed. 2002;30((6)):29–37.

16.	[PubMed] Mubarak, S., Gould, R., Lee, Y., Schmidt, D., & Hargens, A. 1982, " The medial tibial stress syndrome: a cause of shin splints", The American Journal of Sports Medicine, Vol. 10, No. 4, pp. 201-205.

17.	Brukner P. Exercise related lower leg pain: bone. Med Sci Sports Exerc. 2000;32((suppl 3)):15S–26S. [PubMed]

18. Beck B.R, Osternig L.R. Medial tibial stress syndrome: the location of muscles in the leg in relation to symptoms. J Bone Joint Surg Am. 1994;76((7)):1057–1061. [PubMed]

19. Sommer H.M, Vallentyne S.W. Effect of foot posture on the incidence of medial tibial stress syndrome. Med Sci Sports Exerc. 1995;27((6)):800–804. [PubMed]

20. Beck B.R. Tibial stress injuries: an aetiological review for the purposes of guiding management. Sports Med. 1998;26((4)):265–279. [PubMed]

21. Reinking M.F, Hayes A.M. Intrinsic factors associated with exercise-related leg pain in collegiate cross-country runners. Clin J Sport Med. 2006;16((1)):10–14. [PubMed]

22. Bennett J.E, Reinking M.F, Pluemer B, Pentel A, Seaton M, Killian C. Factors contributing to the development of medial tibial stress syndrome in high school runners. J Orthop Sports Phys Ther. 2001;31((9)):504–510. [PubMed]

23. PhysioRoom.com. 2013, Shin splints in depth: aka medial tibial stress syndrome, [online] available at: http://www.physioroom.com/injuries/calf_and_shin/shin_splints_full.php [accessed February 25, 2014].

24. Michael, R., & Holder, L. 1985, " Soleus Syndrome – a cause of medial tibial stress (shin splints)" , The American Journal of Sports Medicine, Vol. 13, No. 2, pp. 87 – 94.

25. Newman, P., Adams, R., & Waddington, G. 2011, "Two simple clinical tests for predicting onset of medial tibial stress syndrome: shin palpation test and shin oedema test", British Journal of Sport Medicine, Vol. 46, pp. 861-864.

26. Batt, M. 2011, "Medial Tibial Stress Syndrome", British Journal of Sports Medicine", Vol. 45, pp. e2.

27.   Stickley, C., Hetzler, R., Kimura, I, & Lozanoff, S. 2009, " Crural fascia and muscle origins related to medial tibia stress syndrome, symptom location", Medicine and Science in Sports and Exercise, Vol. 41, No. 11, pp. 1991-1996.

28.   Rathleff, M., Samani, A., Olesen, C., Kersting, U., Madeline, P. 2011, " Inverse relationship between the complexity of midfoot kinematics and muscle activation in patients with medial tibial stress syndrome", Journal of Electromyography and Kinesiology, Vol. 21, pp. 638-644.

29.   Craig, D. I. (2008). Medial tibial stress syndrome: evidence-based prevention.Journal of athletic training, 43(3), 316.

30.   Andrish JT: The shin splint syndrome. In Orthopaedic sports medicine chapter 29.. 2 edition. Edited by: DeLee JC, Drez D. Amsterdam: Elsevier; 2003:2155-2158.

31.   Kortebein PM, Kaufman KR, Basford JR, Stuart MJ: Medial tibial stress syndrome. Med Sci Sports Exerc 2000, 32(Suppl. 3):S27-S33.

32.   Kaspar D, Seidl W, Neidlinger-Wilke C, Claes L: In vitro effect of dynamic strain on the proliferative and metabolic activity of human osteoblasts. J Musculoskel Neuron Interact 2000, 1(2):161-164.

33.   Lozupone E, Palumbo C, Favia A, Ferretti M, Palazzini F, Cantatore FP: Intermittent compressive load stimulates osteogenesis and improves osteocytes viability in bones cultured in vitro. Clin Rheumatol 1996, 15(6):563-572.

34.   Waldorff EI, Christenson KB, Cooney LA, Goldstein SA: Microdamage repair and remodeling requires mechanical loading. J Bone Miner Res 2010, 25(4):734-745.

35.   Hill DB: Production and absorption of work by muscle. Science 1960, 131(3404):897-903.

36. Paul IL, Murno MB, Abernethy PJ, Simon SR, Radin EL, Rose RM: Musculoskeletal shock absorption: relative contribution of bone and soft tissues at various frequencies. J Biomech 1978, 11(5):237-239.

37. Radin EL: Role of muscles in protecting athletes from injury. Acta Med Scand Suppl 1986, 711:143-147.

38. Winter DA: Moments of force and mechanical power in jogging. J Biomech 1983, 16(1):91-97.

39. Meardon, S. A. (2009). Skeletal loading: implications for injury and treatment.

40. Zimmermann WO, Paantjes MA: Sport compression stockings: user satisfaction 50 military personnel. Dutch J Mil Med 2009, 62:209-213.

41. Roelofsen J, Klein-Nulend J, Burger EH: Mechanical stimulation by intermittent hydrostatic compression promotes bone-specific gene expression in vitro. J Biomech 1995, 33(12):1493-1503.

42. Blackburn, M. H. (2002). A Prospective Design Identifying Etiological Risk Factors Associated with MTSS and Stress Fractures in Female Intercollegiate Athletes.

43. Moen et al. Sports Medicine, Arthroscopy, Rehabilitation, Therapy & Technology 2012, 4:12

44. Stickley, C. D., Hetzler, R. K., Kimura, I. F., & Lozanoff, S. C. O. T. T. (2009). Crural fascia and muscle origins related to medial tibial stress syndrome symptom location. Medicine and science in sports and exercise, 41(11), 1991-1996.

45. O'Connor KM, et al. Clin Biomech (Bristol , Avon) 2004 Jan; 19(1): 71-7.

46. Bouche RT, et al. J Am Podiatr Med Assoc 2007 Jan; 97(1): 31-6.

47.   Dar, F. H., Meakin, J. R., & Aspden, R. M. (2002). Statistical methods in finite element analysis. Journal of biomechanics, 35(9), 1155-1161.

48.   Mburu, G., Aspden, R.M., Hutchison, J.D., 1999. Optimising the configuration of cement keyholes for acetabular fixation in total hip replacement using taguchi experimental design. Proceedings of the Institution of Mechanical Engineers. Part H—Journal of Engineering in Medicine 213 (6), 485–492.

49.   Taguchi, G., 1987. System of Experimental Design. UNIPUB Kraus International Publications, New York.

48.   Beckett ME, Massie DL, Bowers KD, Stoll DA. Incidence of hyperpronation in the ACL injured knee: A clinical perspective. J Athlet Train 1992;27:58-62.

49.   Loudon JK, Jenkins W, Loudon KL. The relationship between static posture and ACL injury in female athletes. J Orthop Sports Phys Ther 1996;24:91-7.

50.   Delacerda FG. A study of anatomical factors involved in shin splints. J Orthop Sports Phys Ther 1980;2:55-9.

51.   Brody TM. Techniques in the evaluation and treatment of the injured runner. Orthop Clin North Am 1982;13:541-58.

52.   Vinicombe A, Raspovic A, Menz HB. reliability of navicular displacement measurement as a clinical indicator of foot posture. J Am Podiat Med Assn 2001;91:262-8.

53.   Plisky, M., Rauh, M., Heiderscheit, B., Tank, R., & Underwood, F. (2007). Medial tibial stress syndrome in high school cross-country runners: Incidence and risk factors. Journal of Orthopaedic & Sports Physical Therapy, 37(2), 40-47.

54.   Gajdosik, R. L., & Bohannon, R. W. (1987). Clinical measurement of range of motion review of goniometry emphasizing reliability and validity. Physical Therapy, 67(12), 1867-1872.

55.   Daoud, A. I., Geissler, G. J., Wang, F., Saretsky, J., Daoud, Y. A., & Lieberman, D. E. (2012). Foot strike and injury rates in endurance runners: a retrospective study. Med Sci Sports Exerc, 44(7), 1325-34.

56.   DeWit B, De Clercq D, Aerts P. Biomechanical analysis of the stance phase during barefoot and shod running. J Biomech. 2000;33: 269–78.

57.   Laughton CA, Davis I, Hamill J. Effect of strike pattern and orthotic intervention on tibial shock during running. J Appl Biomech. 2003;19:153–68.

58.   Lieberman DE, Venkadesan M, Werbel WA, et al. Foot strike patterns and collision forces in habitually barefoot versus shod runners. Nature. 2010;463:531–5.

59.   Loudon, J. K., & Reiman, M. P. (2012). Lower extremity kinematics in running athletes with and without a history of medial shin pain. International journal of sports physical therapy, 7(4), 356.

60.   King, J. (2013). Association between overuse injury and biomechanics in distance runners (Doctoral dissertation, Wake Forest University).

61.   Olesen, C. G., Andersen, M. S., Rathleff, M. S., de Zee, M., & Rasmussen, J. (2009, June). Understanding the biomechanics of medial tibial stress syndrome: a simulation study using a musculoskeletal model. In Congress of the International Society of Biomechanics, ISB.

62.	Al Nazer, R., Rantalainen, T., Heinonen, A., Sievänen, H., & Mikkola, A. (2008). Flexible multibody simulation approach in the analysis of tibial strain during walking. Journal of biomechanics, 41(5), 1036-1043.

63.	Geraldes, D. M., & Phillips, A. (2014). A comparative study of orthotropic and isotropic bone adaptation in the femur. International journal for numerical methods in biomedical engineering, 30(9), 873-889.

64.	Huiskes R, Weinans H, Grootenboer H, Dalstra M, Fudala B, Sloof T. Adaptative bone-remodelling theory applied to prosthetic-design analysis. Journal of Biomechanics 1987; 20(11/12):1135–1150. DOI: 10.1016/0021-9290(87)90030-3.

65.	Beaupré G, Orr T, Carter D. An approach for time-dependent bone modelling and remodelling—theoretical development. Journal of Orthopaedic Research 1990a; 8:651–661.

66.	Beaupré G, Orr T, Carter D. An approach for time-dependent bone modelling and remodelling—application: a preliminary remodelling situation. Journal of Orthopaedic Research 1990b; 8:662–670.

67.	Weinans H, Huiskes R, Grootenboer HJ. The behaviour of adaptive bone-remodeling simulation models. Journal of Biomechanics 1992; 25(12):1425–1441.

68.	Folgado J, Fernandes PR, Guedes JM, Rodrigues HC. Evaluation of osteoporotic bone quality by a computational model for bone remodeling. Computers & Structures 2004; 82(17–19):1381–1388. DOI: 10.1016/j.compstruc.2004.03.033.

69.	García-Aznar JM, Rueberg T, Doblaré M. A bone remodelling model coupling micro-damage growth and repair by 3D BMU-activity. Biomechanics and Modeling in Mechanobiology 2005; 4(2–3):147–67. DOI: 10.1007/s10237-005-0067-x.

70. Rho JY, RoyME, II, Tsui TY, Pharr GM. Elastic properties of human cortical and trabecular lamellar bone measured by nanoindentation. Biomaterials 1997; 18:1325–1330. DOI: 10.1016/S0142-9612(97)00073-2.

71. Coelho PG, Fernandes PR, Rodrigues HC, Cardoso JB, Guedes JM. Numerical modeling of bone tissue adaptation—a hierarchical approach for bone apparent density and trabecular structure. Journal of Biomechanics 2009;42(7):830–837. DOI: 10.1016/j.jbiomech.2009.01.020.

72. Kowalczyk P. Simulation of orthotropic microstructure remodelling of cancellous bone. Journal of Biomechanics 2010; 43:563–569. DOI: 10.1016/j.jbiomech.2009.09.045.

73. Hambli R, Rieger R. Physiologically based mathematical model of transduction of mechanobiological signals by osteocytes. Biomechanics and Modeling in Mechanobiology 2012; 11(1–2):83–93. DOI: 10.1007/s10237-011-0294-2.

74. Rieger R, Hambli R, Jennane R. Modeling of biological doses and mechanical effects on bone transduction. Journal of Theoretical Biology 2011; 274(1):36–42. DOI: 10.1007/s10237-011-0294-2.

75. Campoli G, Weinans H, Zadpoor AA. Computational load estimation of the femur. Journal of the Mechanical Behavior of Biomedical Materials 2012; 10:108–119. DOI: 10.1016/j.jmbbm.2012.02.011.

76. Miller Z, Fuchs M, Arcan M. Trabecular bone adaptation with an orthotropic material model. Journal of Biomechanics 2002; 35:247–256. DOI: 10.1016/S0021-9290(01)00192-0.

77. Ashman R, Cowin S, van Buskirk W, Rice J. A continuous wave technique for the measurement of the elastic properties of cortical bone. Journal of Biomechanics 1984; 17:349–361. DOI: 10.1016/0021-9290(84)90029-0.

78. Cuppone M, Seedhiom B, Berry E, Ostell A. The longitudinal Young's modulus of cortical bone in the midshaft of human femur and its correlation with CT scanning data. Calcified Tissue International 2004; 74:302–309. DOI: 10.1007/s00223-002-2123-1.

79. Turner C, Rho J, Takano Y, Tsui T, Pharr G. The elastic properties of trabecular and cortical bone tissues are similar: results from two microscopic measurement techniques. Journal of Biomechanics 1999; 32:437–441. DOI: 10.1016/S0021-9290(98)00177-8.

80. Garden RS. The structure and function of the proximal end of the femur. Journal of Bone and Joint Surgery—British Volume 1961; 43-B(3):576–589.

81. Singh M, Nagrath AR, Maini PS. Changes in trabecular pattern of the upper end of the femur as an index of osteoporosis. Journal of Bone and Joint Surgery 1970; 52:457–467.

82. Skedros J, Baucom S. Mathematical analysis of trabecula 'trajectories' in apparent trajectorial structures: the unfortunate historical emphasis on the human proximal femur. Journal of Theoretical Biology 2007; 244:15–45. DOI: 10.1016/j.jtbi.2006.06.029.

83. Wolff J. The Law of Bone Remodelling. Springer-Verlag: Berlin, 1892.

84. Rohrbach D, Lakshmanan S, Peyrin F, Langer M, Gerisch A, Grimal Q, Laugier P, Raum K. Spatial distribution of tissue level properties in a human femoral cortical bone. Journal of Biomechanics 2012; 45(13):2264–2270. DOI: 10.1016/j.jbiomech.2012.06.003.

85. Vuong J, Hellmich C. Bone fibrillogenesis and mineralization: quantitative analysis and implications for tissue elasticity. Journal of Theoretical Biology 2011; 287:115–30. DOI: 10.1016/j.jtbi.2011.07.028.

86.   Blanchard R, Dejaco A, Bongaers E, Hellmich C. Intravoxel bone micromechanics for microCT-based finite element simulations. Journal of Biomechanics 2013; 46(15):2710–2721. DOI: 10.1016/j.jbiomech.2013.06.036.

87.   Hellmich C, Kober C, Erdmann B. Micromechanics-based conversion of CT data into anisotropic elasticity tensors, applied to FE simulations of a mandible. Annals of Biomedical Engineering 2008; 36(1):108–122. DOI: 10.1557/PROC-1132-Z01-03.

88.   Yosibash Z, Trabelsi N, Hellmich C. Subject-specific p-FE analysis of the proximal femur utilizing micromechanics based material properties. International Journal for Multiscale Computational Engineering 2008; 6(5):483–498. DOI: 10.1615/IntJMultCompEng.v6.i5.70.

89.   Taylor, W. R., Roland, E., Ploeg, H., Hertig, D., Klabunde, R., Warner, M. D., ... & Clift, S. E. (2002). Determination of orthotropic bone elastic constants using FEA and modal analysis. Journal of Biomechanics, 35(6), 767-773.

90.   Fregly, B.J., Besier, T.F., Lloyd, D.G., Delp, S.L., Banks, S.A., Pandy, M.G., and D'Lima, D.D. Grand challenge competition to predict in vivo knee loads. Journal of Orthopaedic Research 30(4):503-513 (2012).\

91.   Wong, C., Mikkelsen, P., Hansen, L. B., Darvann, T., & Gebuhr, P. (2010). Finite element analysis of tibial fractures. Dan Med Bull, 57(5), A4148.

92.   Ionescu, I., Conway, T., Schonning, A., Almutairi, M., & Nicholson, D. W. (2003). Solid modeling and static finite element analysis of the human tibia. In Sonesta Beach Resort in Key Biscayne, Florida, June. Summer Bioengineering Conference, 25 (Vol. 29).

93. Li, Q., Steven, G. P., & Xie, Y. M. (1999). On equivalence between stress criterion and stiffness criterion in evolutionary structural optimization. Structural optimization, 18(1), 67-73.

94. Chamis, C.C., and Sinclair, J.H., "10° Off-Axis Test for Intralaminar Shear Characterization of Fiber Composites," Report TN D-8215, NASA-Lewis Research Center (Cleveland, Ohio), April 1976.

95. Sheikh-Warak, A. (2012). Comparing Strains in the Tibia induced by different Running Styles: Shod heel striking, minimally shod midfoot striking and barefoot.

96. Lieberman, D. E., Venkadesan, M., Werbel, W. A., Daoud, A. I., D'Andrea, S., Davis, I. S., Mang'Eni, R. O. and Pitsiladis, Y. (2010), `Foot strike patterns and collision forces in habitually barefoot versus shod runners', Nature 463, 531{535.

97. Galbraith, R. M., & Lavallee, M. E. (2009). Medial tibial stress syndrome: conservative treatment options. Current reviews in musculoskeletal medicine, 2(3), 127-133.

98. Beck B. Tibial stress injuries: an aetiological review for the purposes of guiding management. Sports Med. 1998;26(4):265–79.

99. Anderson M, Ugalde V, Batt M, Gacayan J. Shin splints: MR appearance in a preliminary study. Radiology. 1997;204:177–80.

100. Detmer D. Chronic shin splints. Classification and management of medial tibial stress syndrome. Sports Med. 1986;3(6):436–46.

101. Fredericson M, Bergman G, Hoffman K, Dillingham M. Tibial stress reaction in runners: correlation of clinical symptoms and scintigraphy with a new magnetic resonance imaging grading system. Am J Sports Med. 1995;23:427–81.

102. Hoopes, D. M. (2013). Chronic Injuries Due to Running and a Possible Cure with the Barefoot Style. UNM Orthopaedic Research Journal, 2.

103. Willems, T. M., De Clercq, D., Delbaere, K., Vanderstraeten, G., De Cock, A., & Witvrouw, E. (2006). A prospective study of gait related risk factors for exercise-related lower leg pain. Gait & posture, 23(1), 91-98.

104. Altman, A., & Davis, D. (2012). Comparison of tibial strains and strain rates and barefoot and shod running. American Society of Biomechanics.

105. Kulin et al., J Mech Behav Biomed Mater 4 57-75, 2011.

106. Austman J Biomech 41(15), 3171-3176, 2008

107. Hall, J. (2010). Dynamic Simulation and Collision Modeling of the Packbot Manipulator (No. TARDEC-21387). AUTOMOTIVE RESEARCH CENTER ANN ARBOR MI.

108. Riviere, B., Shaw, S., Wheeler, M. F., & Whiteman, J. R. (2003). Discontinuous Galerkin finite element methods for linear elasticity and quasistatic linear viscoelasticity. Numerische Mathematik, 95(2), 347-376.

109. Horsman, M. K., Koopman, H., van der Helm, F., Prose, L. P. and Veeger, H. (2007), `Morphological muscle and joint parameters for musculoskeletal modelling of the lower extremity', Cl 22, 239{247.

110. Wang, N., & Liu, Y. H. (2004). Application of Taguchi's design of experiments to the study of biomechanical systems. Journal of Applied Biomechanics, 20, 219-229.

111. Brekelmans, W. A. M., Poort, H. W., & Slooff, T. J. J. H. (1972). A new method to analyse the mechanical behaviour of skeletal parts. Acta Orthopaedica, 43(5), 301-317.

112.   Gray, H. A., Taddei, F., Zavatsky, A. B., Cristofolini, L., & Gill, H. S. (2008). Experimental validation of a finite element model of a human cadaveric tibia. Journal of biomechanical engineering, 130(3), 031016.

113.   Donahue, T. L. H., Hull, M. L., Rashid, M. M., & Jacobs, C. R. (2002). A finite element model of the human knee joint for the study of tibio-femoral contact. Journal of biomechanical engineering, 124(3), 273-280.

114.   Olesen, C. G., Andersen, M. S., Rathleff, M. S., de Zee, M., & Rasmussen, J. (2009, June). Understanding the biomechanics of medial tibial stress syndrome: a simulation study using a musculoskeletal model. In Congress of the International Society of Biomechanics, ISB.

115.   Burr, D. B., Milgrom, C., Fyhrie, D., Forwood, M., Nyska, M., Finestone, A., ... & Simkin, A. (1996). In vivo measurement of human tibial strains during vigorous activity. Bone, 18(5), 405-410.